Sources of Beam Instability

- Magnetic Field Errors

- Mechanical

Sources of Beam Instability - Magnetic Field Errors

A localized change in transverse magnetic field $\delta B(s)$ will introduce a kick

$$\Delta x' = \frac{1}{B\rho}\int \delta B(s)\,ds$$

which in turn will cause a closed orbit distortion with a kink in it:

$$\Delta x(s) = \frac{\sqrt{\beta_x(s)\beta_1}\,\Delta x_1'}{2\sin\pi\nu_x}\cos[\psi_x(s) - \psi_x(s_1) + \nu_x\pi] \quad s < s_1$$

$$= \frac{\sqrt{\beta_x(s)\beta_1}\,\Delta x_1'}{2\sin\pi\nu_x}\cos[\psi_x(s_1) - \psi_x(s) + \nu_x\pi] \quad s > s_1$$

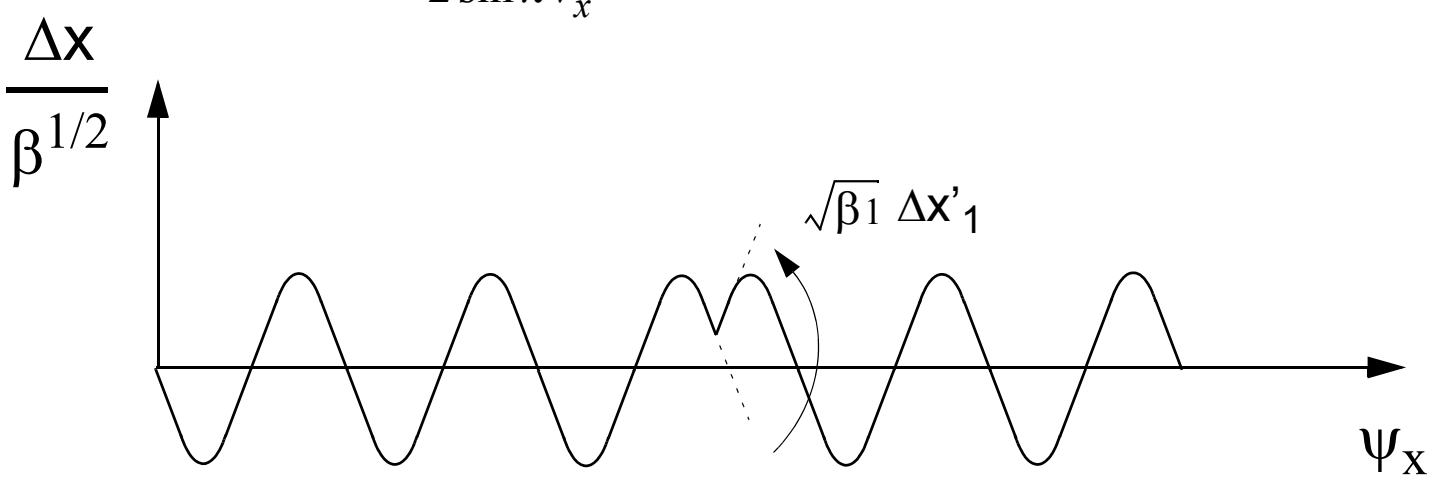

Sources of Beam Instability - Quadrupole Magnetic Field Errors

Table 1 - Quadrupole Parameters

Strength	20	T/m
Bore Diameter	80	mm
Effective Length	0.8	m
Turns/pole	33	
Conductor Height	11.5	mm
Width	11.5	mm
Hole Diameter	6.3	mm
Inductance	29	mH
Resistance	45	mΩ
Current	414	A
Current Density in Coil	2.5	A/mm^2
Voltage	19	V
Power	7.9	kW
Water Flow	2.7	gal/min
Water Pressure Drop	40	psi
Water Temperature Rise	11	°C

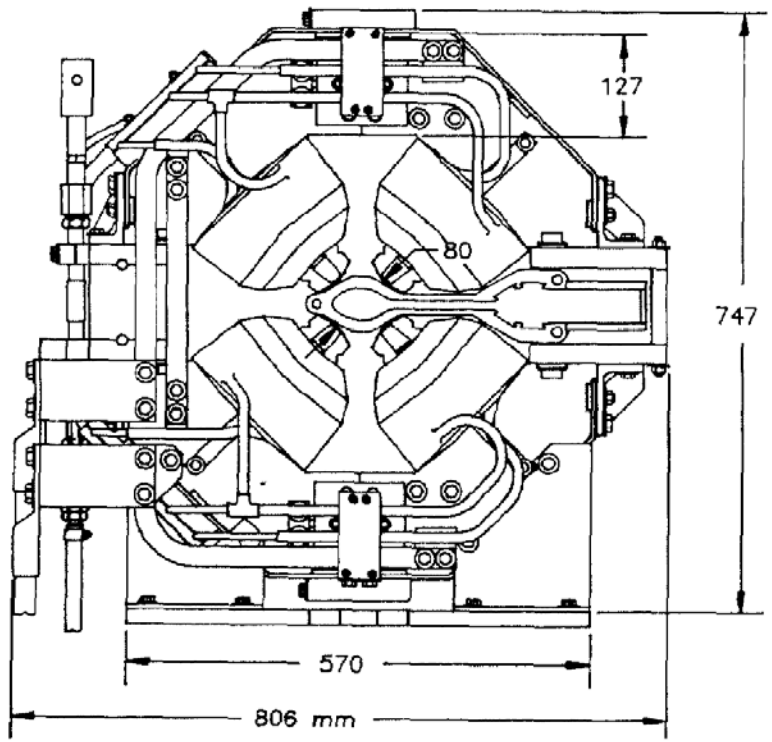

K. Thompson etal, http://accelconf.web.cern.ch/accelconf/p89/PDF/PAC1989_0396.PDF

Quadrupole Magnetic Field

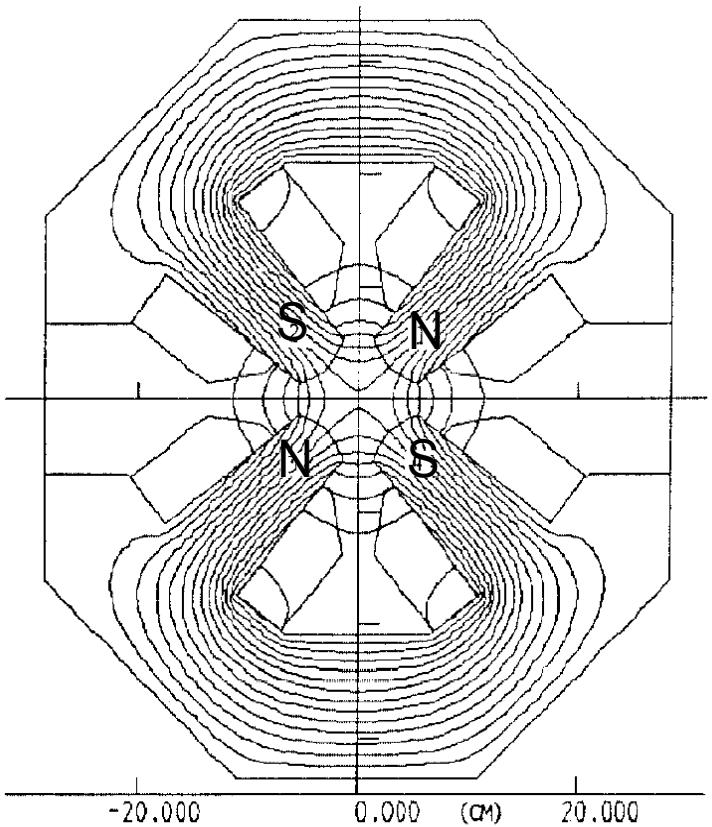

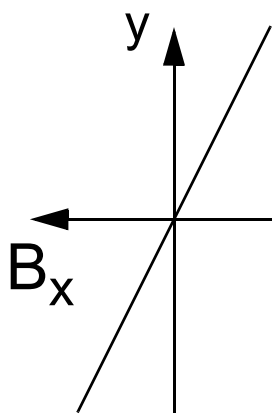

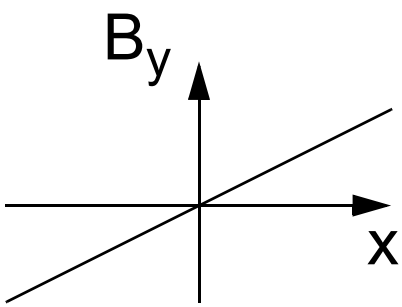

Quadrupole Magnetic Focussing Properties

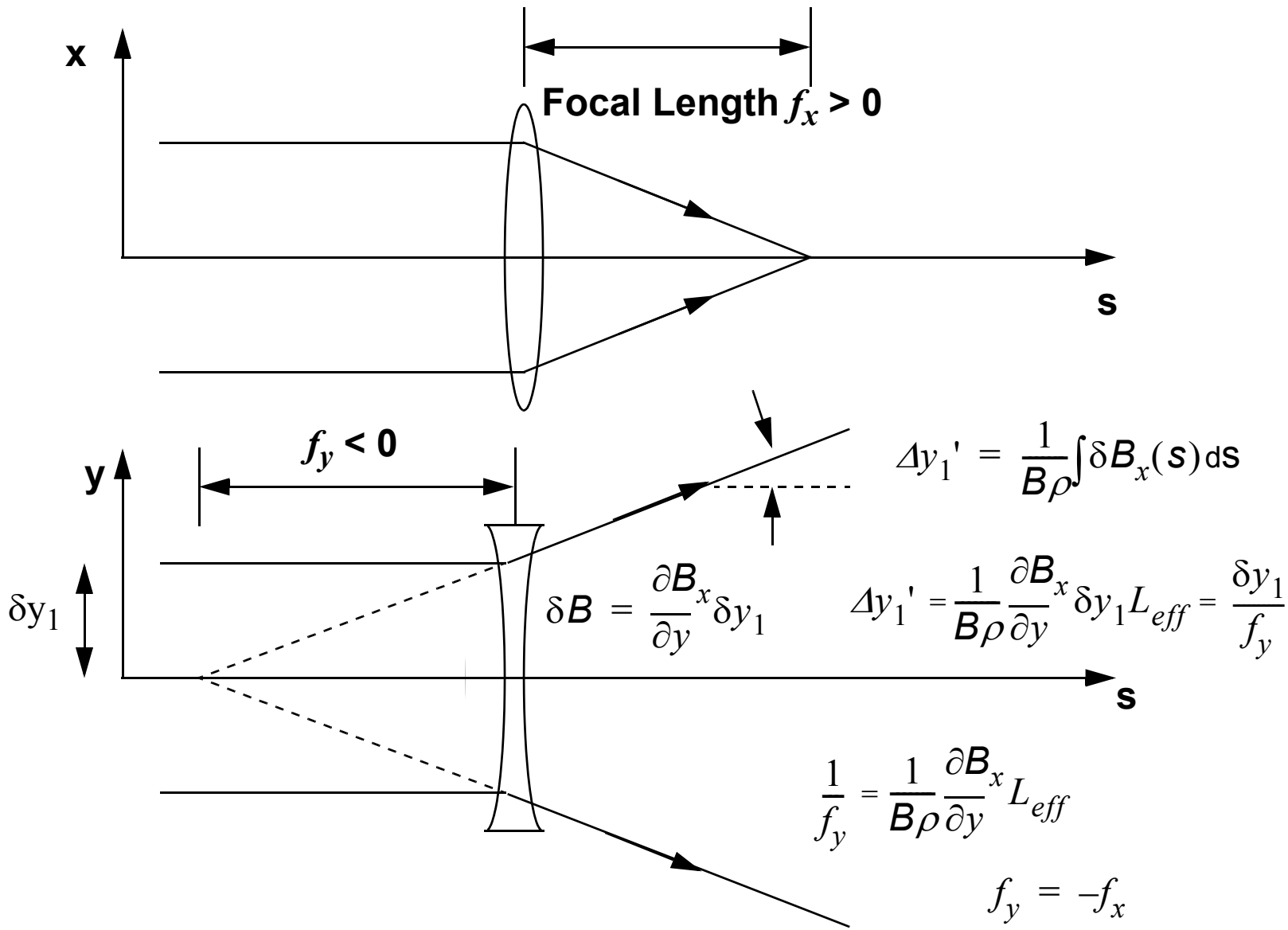

$$\Delta y_1' = \frac{1}{B\rho}\int \delta B_x(s)\,ds$$

$$\delta B = \frac{\partial B_x}{\partial y}\delta y_1$$

$$\Delta y_1' = \frac{1}{B\rho}\frac{\partial B_x}{\partial y}\delta y_1 L_{eff} = \frac{\delta y_1}{f_y}$$

$$\frac{1}{f_y} = \frac{1}{B\rho}\frac{\partial B_x}{\partial y}L_{eff}$$

$$f_y = -f_x$$

Quadrupole Misalignment Amplification Factor

Closed orbit distortion $\Delta y(s)$ resulting from the misalignment of a quadrupole with focal length f_y by an amount δy_1

$$\Delta y(s) = \frac{\sqrt{\beta_x(s)\beta_1}\,\Delta y_1'}{2\sin\pi\nu_y}\cos[\psi_y(s) - \psi_y(s_1) + \nu_x\pi] \qquad \Delta y_1' = \frac{\delta y_1}{f_y}$$

The cumulative effect of the uncorrelated misalignment of N quadrupole magnets is to produce an rms closed orbit deviation

$$\boxed{\sigma_{co}(s) = \frac{\sqrt{\beta_x(s)\langle\beta\rangle}}{2\sin\pi\nu_x}\frac{\sigma_q}{|f_x|}\sqrt{\frac{N}{2}}}$$

where σ_q is the rms amount of quadrupole misalignment. This formula was derived for a simple FODO lattice, where focussing and defocussing quads have the same focal length, but with opposite sign, although the general behaviour is similar for any storage ring.. The quantity $<\beta>$ is the average beta function at the quadrupole locations.

J. Rossbach, Particle Accelerators, 1998, Vol. 23, pp.121-132

Ramifications of Amplification Factor for Orbit Stabilization

$$\sigma_{co}(s) = \frac{\sqrt{\beta_x(s)\langle\beta\rangle}}{2\sin\pi\nu_x}\frac{\sigma_q}{|f|}\sqrt{\frac{N}{2}}$$

1) Formula is valid for time-dependent quadrupole misalignment, i.e. vibrations

2) Machines with strong focussing (small f --> large field gradient) are potentially very susceptible to large amplification of tiny magnet motions. All modern light sources have extremely strong focussing.

3) It gets worse for larger machines as the square root of N. For APS, N = 400

Design Trick to Fool the Machine

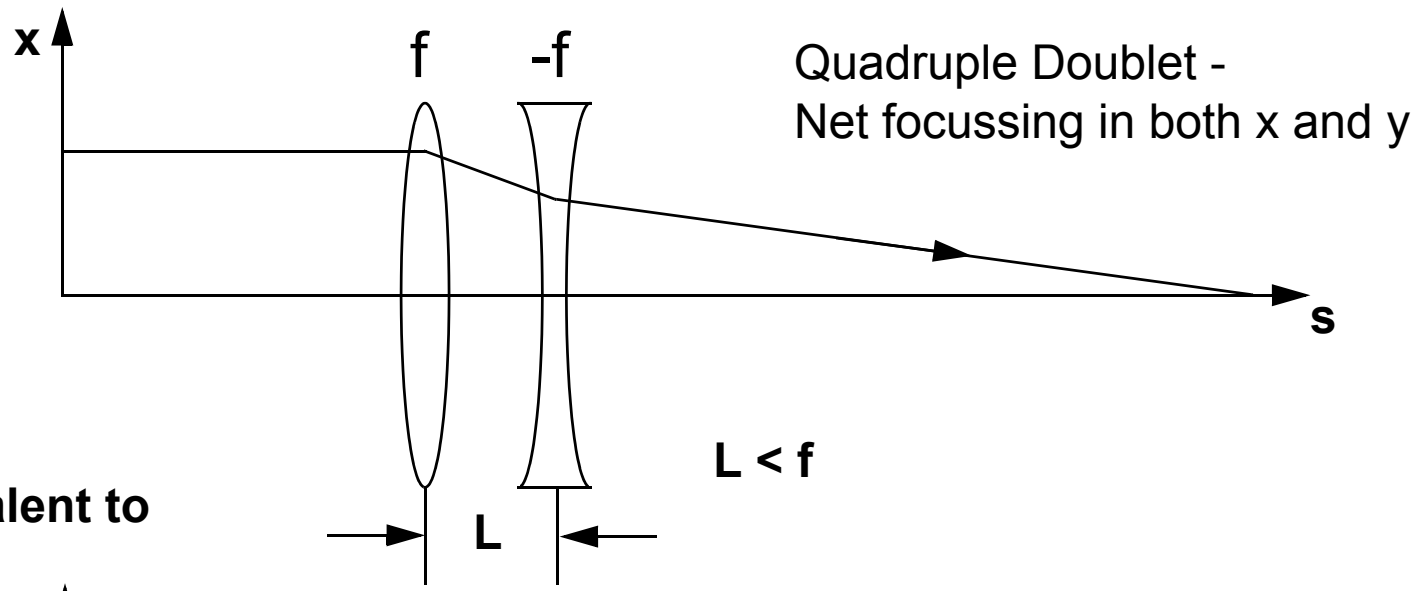

Quadruple Doublet -
Net focussing in both x and y

Equivalent to

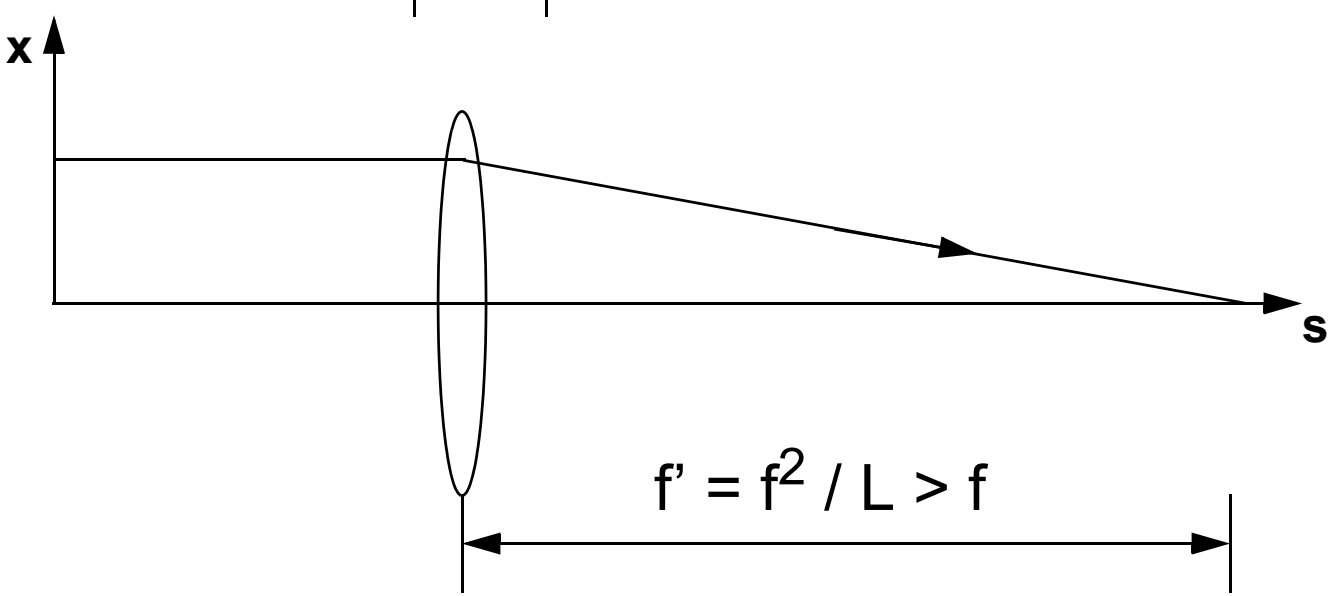

Quadrupole Triplet Mounted Rigidly on a Common Girder

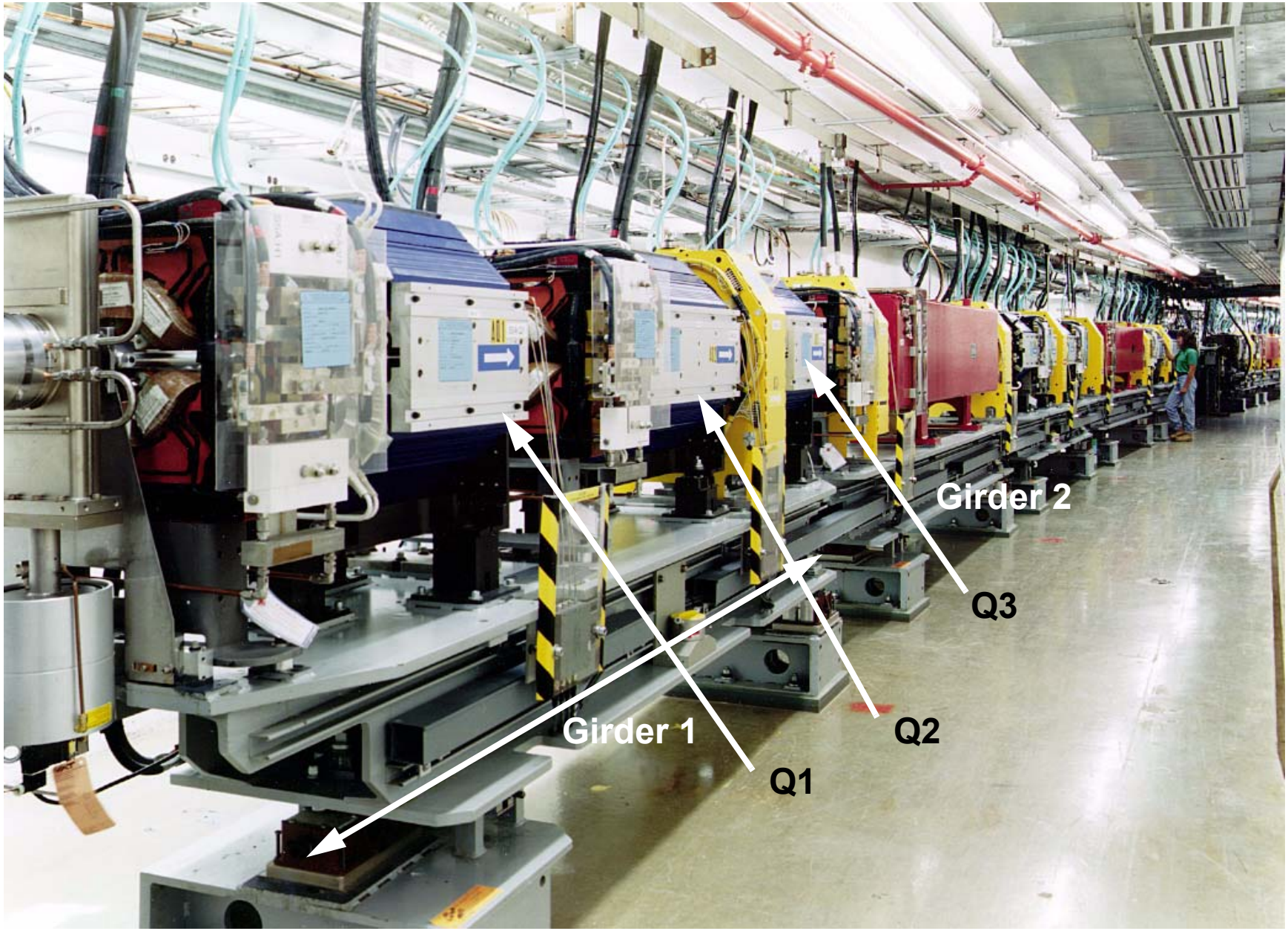

Amplification Factor for Rigidly Mounted Quad Multiplets

$$\sigma_{co}(s) = \frac{\sqrt{\beta_x(s)\langle\beta\rangle}}{2\sin\pi\nu_x}\frac{\sigma_q}{|f|}\sqrt{\frac{N}{2}}$$

Now N = 120 Girders vs. 400 Quadrupoles, $f_{triplet} > f_{quad}$, $\sigma_q \rightarrow \sigma_g$, the rms girder displacement. At the APS, the amplification assuming uncorrelated quadrupole motion was approx. 50 vs. 20 when grouped by girder.

Application of Quadrupole Displacement Formula to Beam-Based Alignment

$$\Delta y(s) = \frac{\sqrt{\beta_x(s)\beta_1}\,\Delta y_1'}{2\sin\pi\nu_y}\cos[\psi_y(s) - \psi_y(s_1) + \nu_x\pi] \qquad \Delta y_1' = \frac{\delta y_1}{f_y}$$

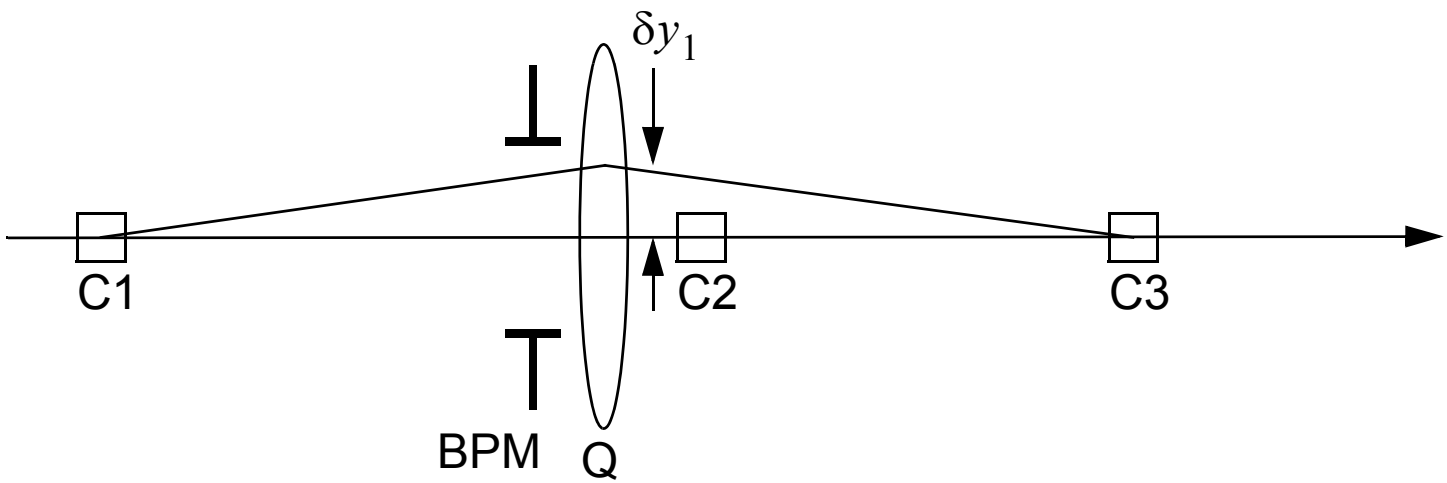

Correctors C1, C2, C3 form a closed bump to vary δy_1

Unless $\delta y_1 = 0$, a small change in the strength of Q will cause a global orbit distortion according to the above formula

Experimental Determination of BPM - Quad Offset

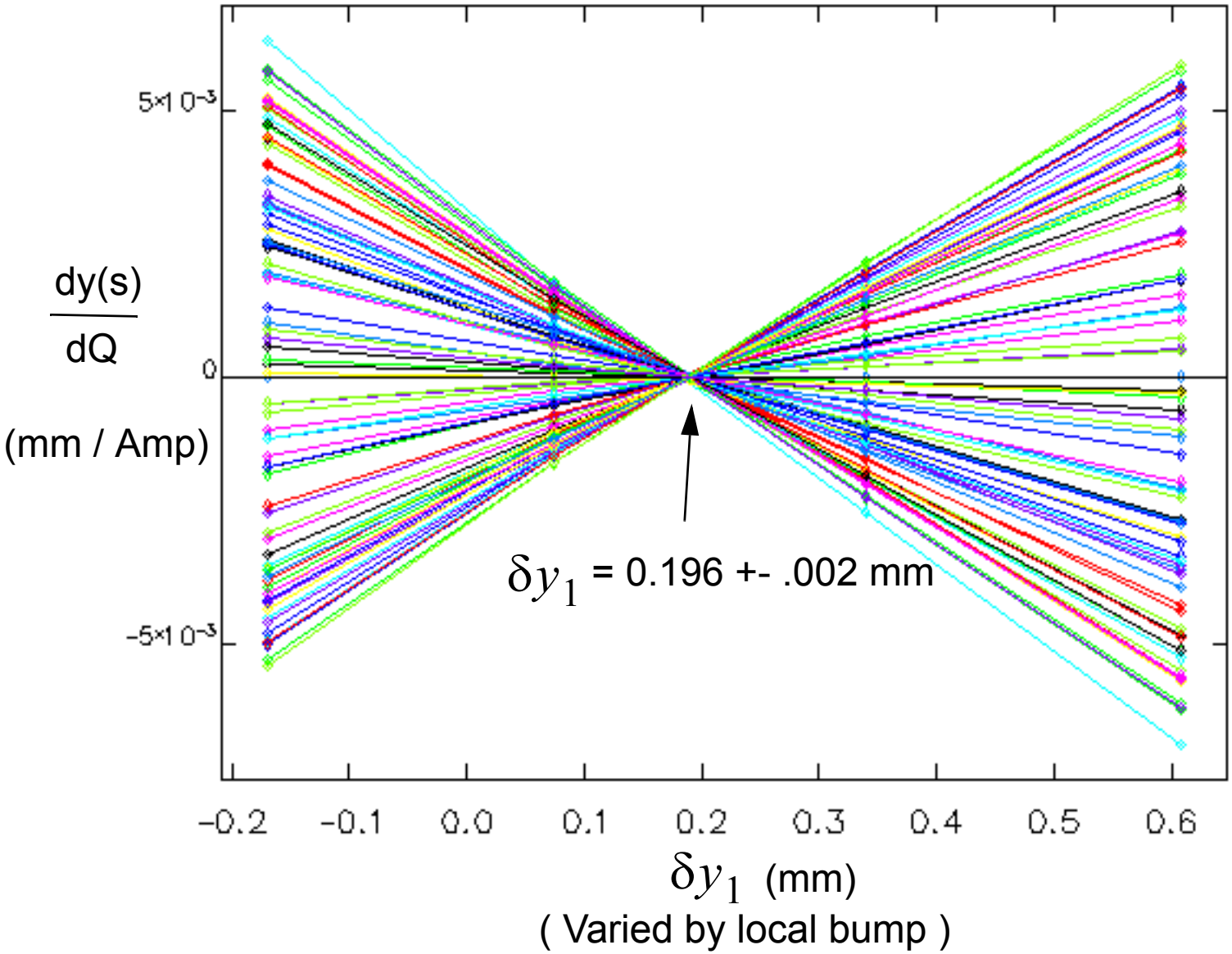

Geophysics

Equation of Motion, Homogenous, Isotropic Media

$$\rho \frac{\partial^2 u_i}{\partial t^2} - (\kappa + \mu) \frac{\partial^2 u_j}{\partial x_i \partial x_j} - \mu \frac{\partial^2 u_i}{\partial x_j^2} = f_i .$$

Ansatz u_i = displacement vector field

$$\vec{u} = \nabla\phi + \nabla \times \vec{\psi} = grad\,\phi + curl\,\vec{\psi},$$

Compressional P-waves

$$\frac{\partial^2 \phi}{\partial t^2} = c^2 \nabla^2 \phi ,$$

Shear S-waves

$$\frac{\partial^2 \vec{\psi}}{\partial t^2} = b^2 \nabla^2 \vec{\psi} ,$$

$c = \sqrt{(\kappa + \frac{4}{3}\mu)/\rho}$ is the P-wave velocity, $b = \sqrt{\mu/\rho}$ is the S-wave velocity.

ρ = mass density - kg / m^3
μ = shear modulus of elasticity
κ = bulk modulus

Ilya Tsvankin, “Seismic Wavefields in Layered Isotropic Media”
Colorado School of Mines Geophyics Dept.

Geometry Associated with Compressional (P) and Shear (S) Waves (Body Waves)

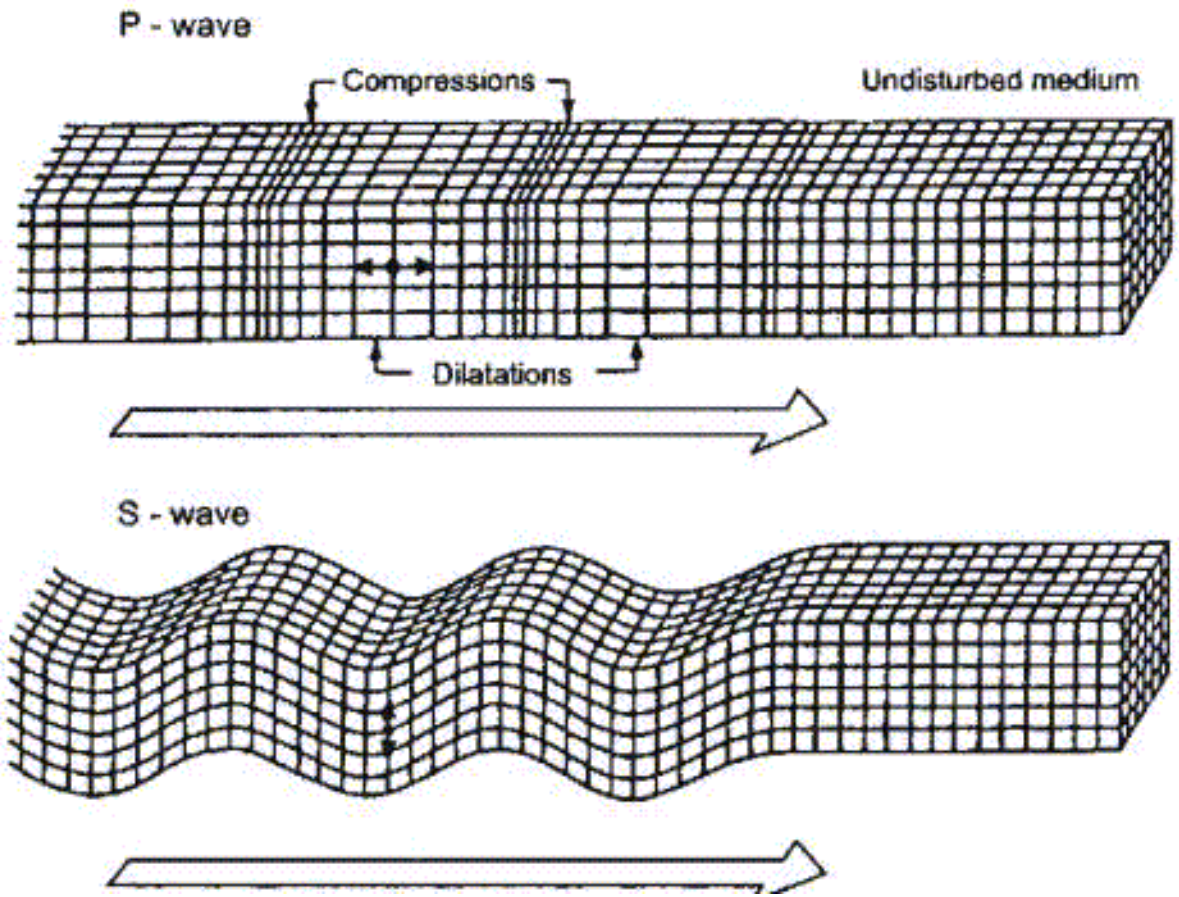

http://www.sfu.ca/earth-sciences/courses/317Spring02/4-Earthquake_Seismology.htm

Yet More Flavors of Seismic Vibrations
(Surface Waves)

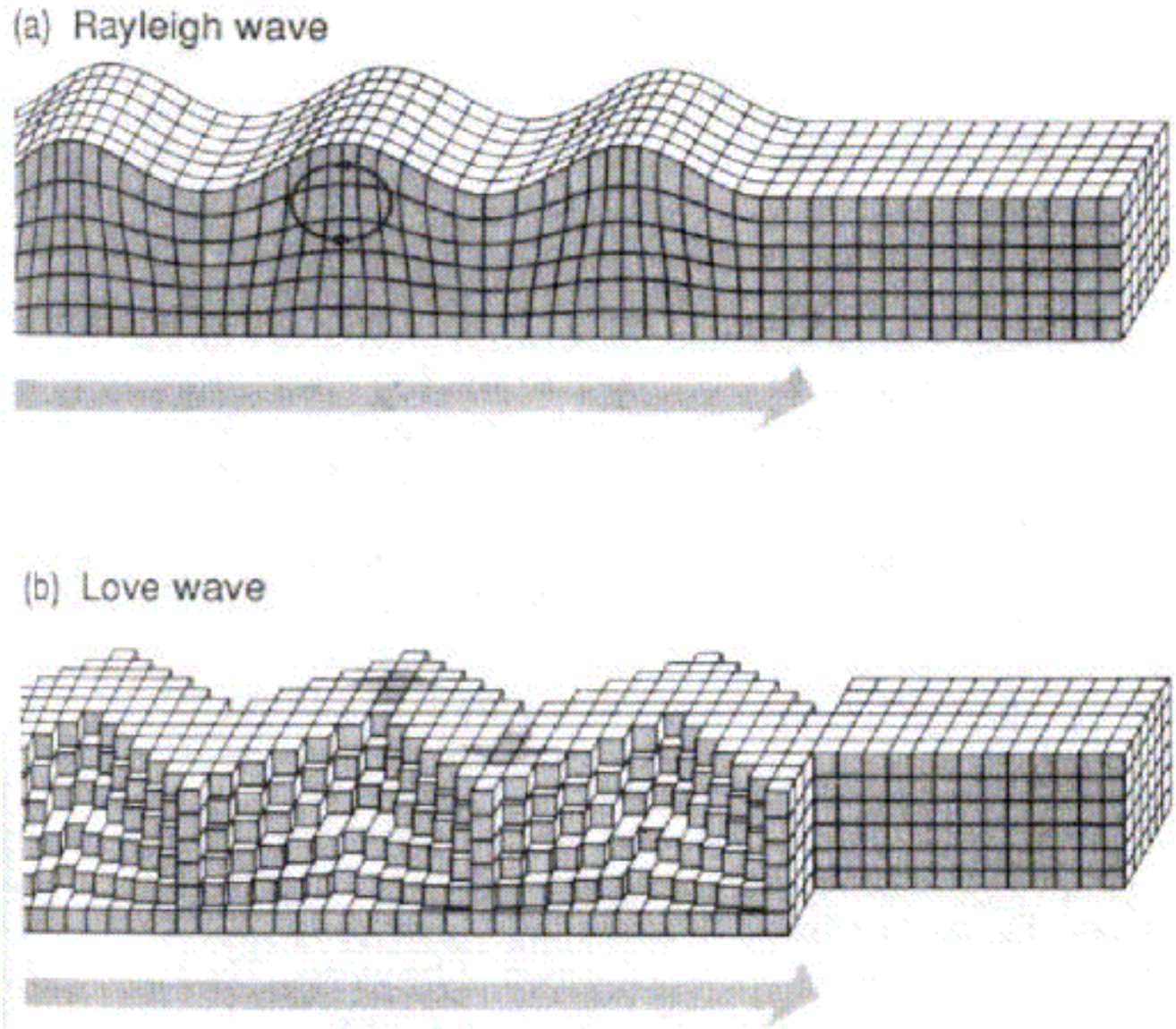

http://www.sfu.ca/earth-sciences/courses/317Spring02/4-Earthquake_Seismology.htm

Material Properties and Seismic Wave Velocities for Various Rock Types

Material	P-wave Velocity C_p (km/s)	S-wave Velocity C_s (km/s)	Bulk Modulus K (GPa)	Rigidity Modulus μ (GPa)	Density ρ (kg/m^3)	Poisson's Ratio σ	Young's Modulus Y (GPa)
Granite	5.5	3.0	49	24	2700	0.29	13.8
Shale	2.2	0.81	9.91	1.64	2500	0.42	1.0
Limestone	6	3	65	24	2700	0.33	14.4
Austin Chalk	2.530	1.219	9.55	3.21	2160	0.35	1.9
Bunter Sandstone	0.76	0.44	0.67	0.40	2080	0.25	1.0

D. Holder, CLRC Daresbury Report AP-BU-rpt-001
http://www.astec.ac.uk/diamond/notes/ap/AP-BU-rpt-001-Ground%20Motion%20Intro.doc

Frequency Scales Associated with Ground Vibration

Machine	**Diameter**	**Revolution Frequency**	**Frequency at which λ = D, @v=750 m/s**
SPEAR	74.6 meters	1.3 MHz	10 Hz
PEP	700 meters	136 kHz	1 Hz
Tevatron	2 km	47 kHz	0.3 Hz

G. Fischer, AIP153, pp. 1047-1119

Accelerator / Ground Motion Resonance Condition

When the wavelength of seismic waves approaches the ring dimensions, an amplification effect takes place whereby the amplitude of closed orbit distortion can be many times larger than the amplitude of ground motion. This resonance condition occurs when

$$\frac{C}{\lambda} = \nu,\ N - \nu,\ N + \nu$$

where C is the ring circumference, N is the number of superperiods, and ν is the fractional part of the tune (vertical or horizontal).

J. Rossbach, Particle Accelerators, 1998, Vol. 23, pp.121-132

Response of Horizontal Beam Position to an Earthquake in Alaska

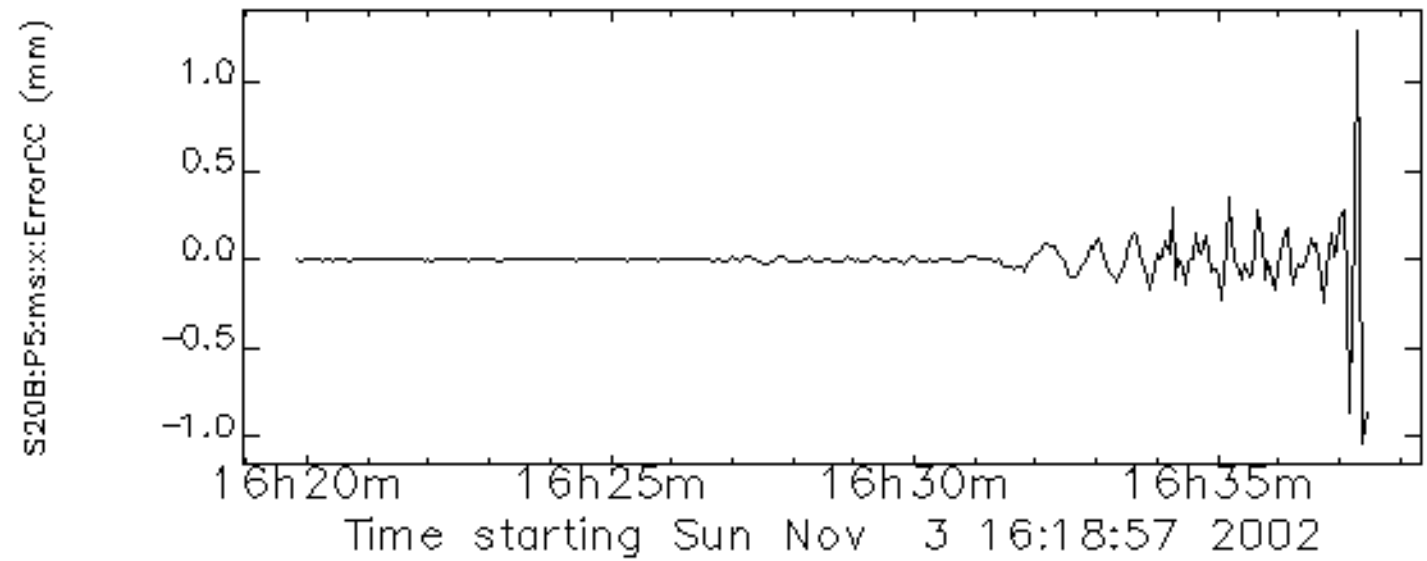

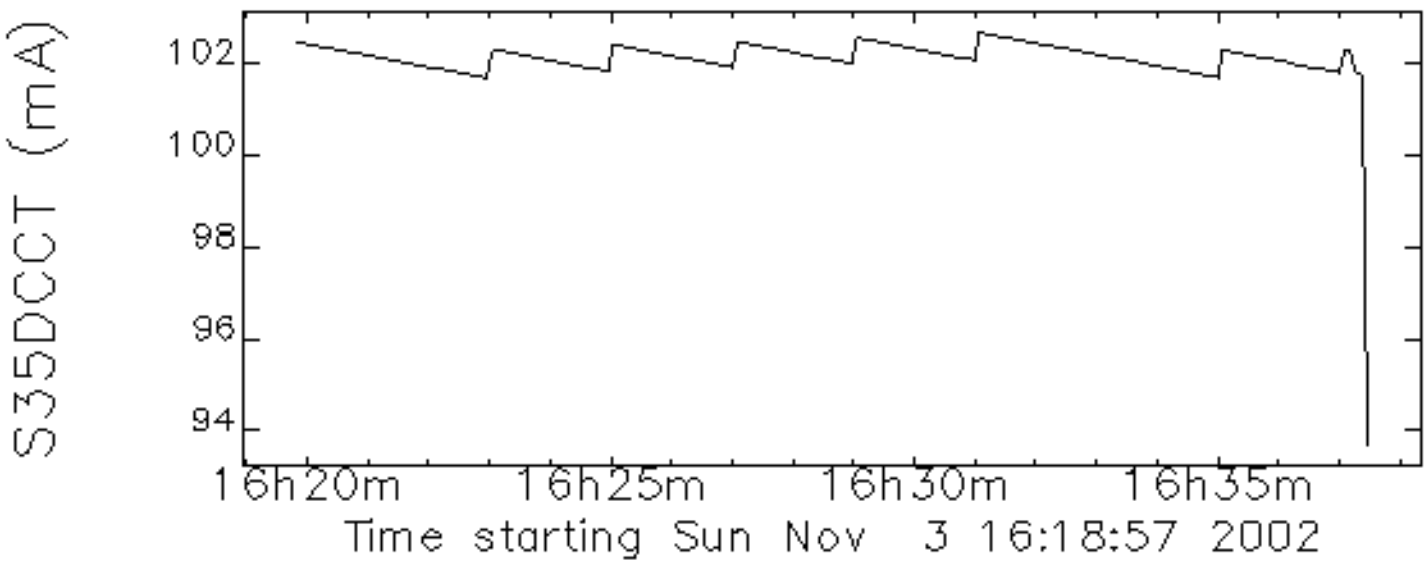

Seismogram of Alaskan Earthquake 11/3/02

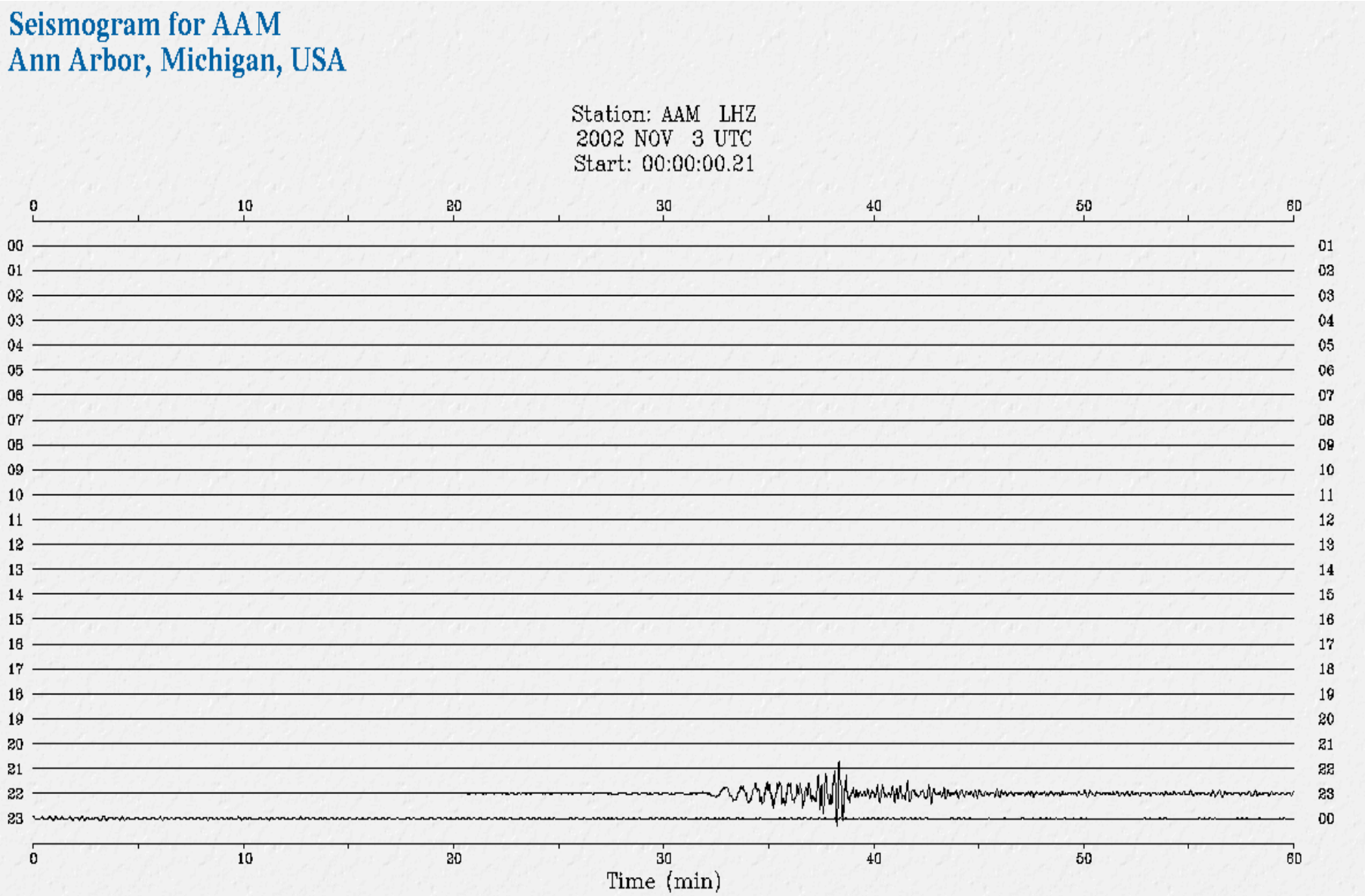

Ground Motion at APS Sector 19 resulting from Driving a Fork Truck Under the Ring

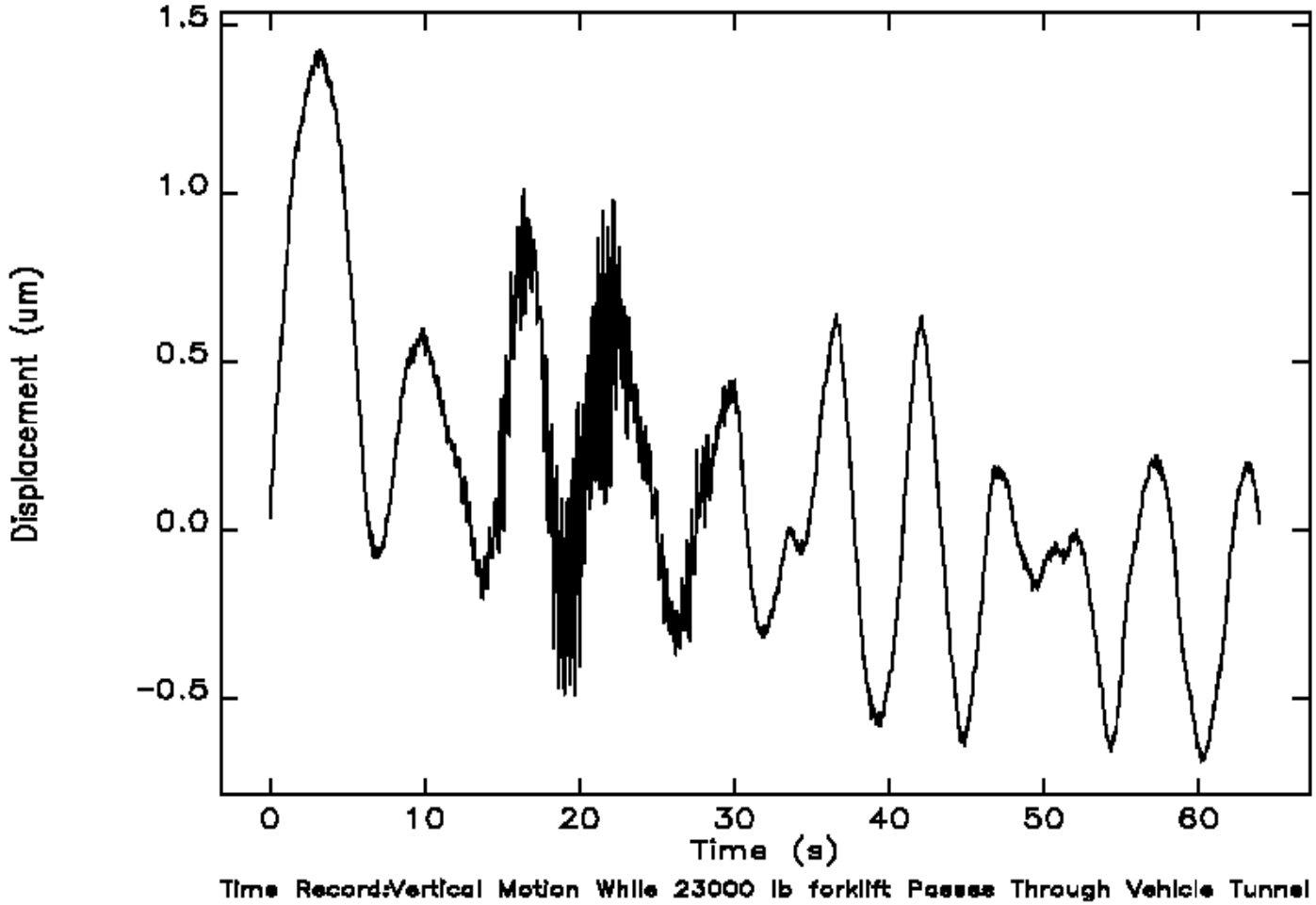

Velocity Power Spectral Density Around the World

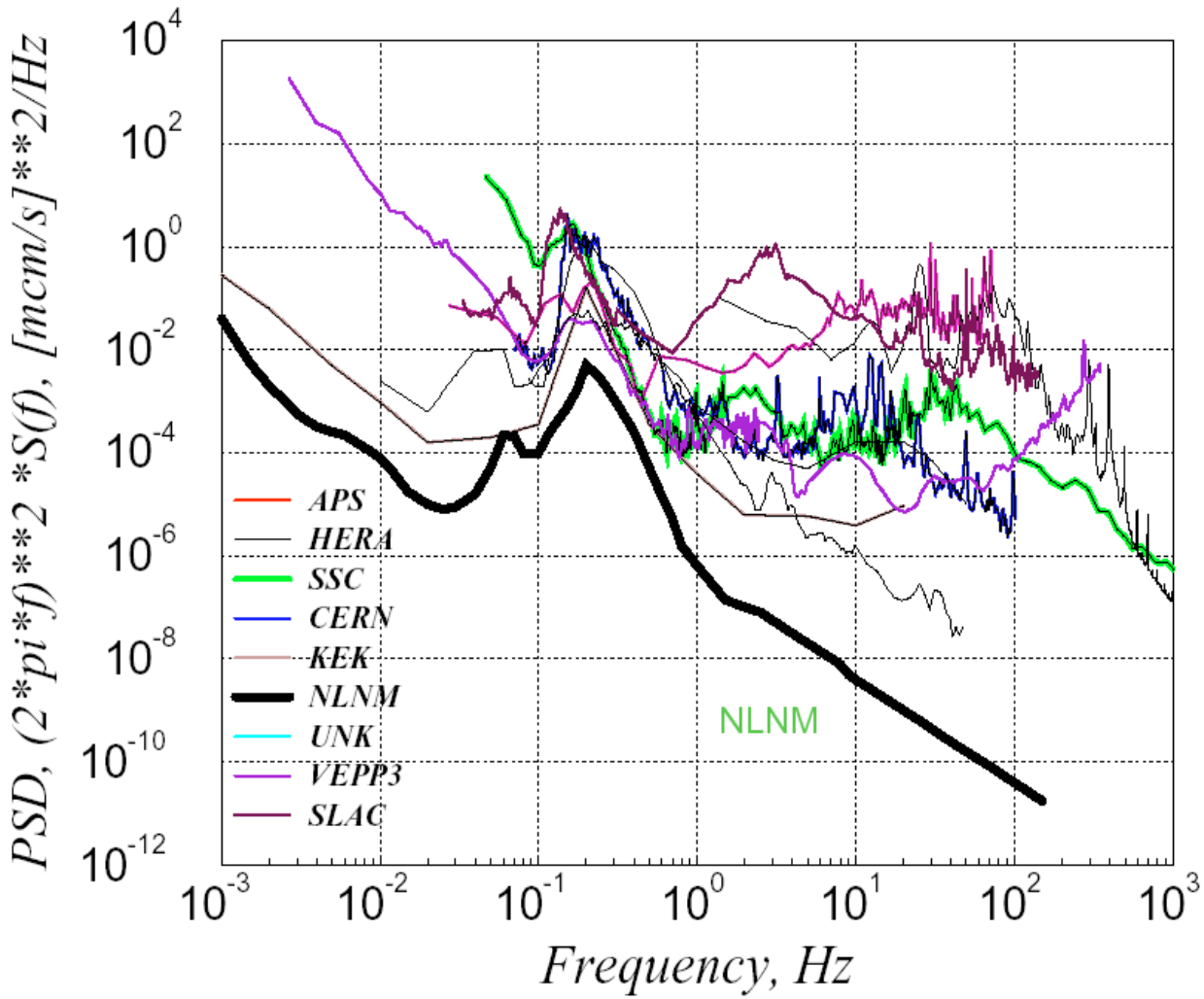

V. Shiltsev, http://epaper.kek.jp/e96/PAPERS/ORALS/TUY03A.PDF

Space-Time Ground Diffusion
(The ATL Law)

The mean square relative displacement (variance) of two points a distance L apart grows linearly with time T according to

$$\langle dX^2 \rangle = ATL$$

where A is on the order of $10^{-5\pm1}$ μm^2 / sec / meter.

This results in power spectral densities in time and space as follows:

$$S_{ATL}(\omega) = \frac{2AL}{\omega^2} \; ; \quad \omega = 2\pi f > 0 \qquad S_{ATL}(k) = \frac{2AT}{k^2} \; ; \quad k = \frac{2\pi}{\lambda} > 0$$

V. Shiltsev, 1995 Workshop on Accelerator Alignment
http://www.slac.stanford.edu/grp/met/TOC_S/1995conf.htm
http://www.slac.stanford.edu/grp/met/TOC_S/Papers/VShil95.pdf

PSD of Closed Orbit Distortion at HERA, Using β = 1 meter

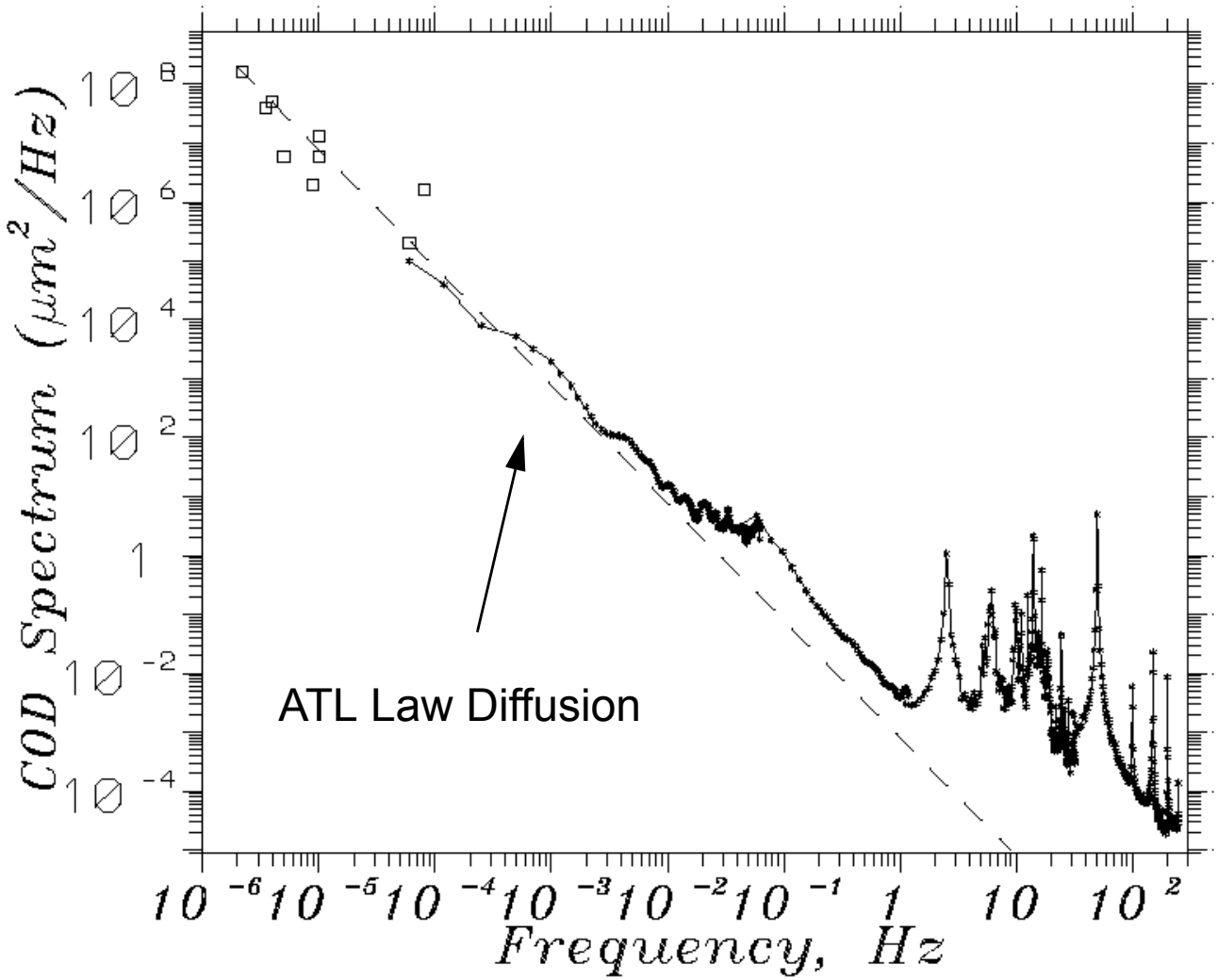

Figure 5: Spectrum of vertical COD at HERA-p.

V. Shiltsev, http://epaper.kek.jp/e96/PAPERS/ORALS/TUY03A.PDF

A Girder - End View

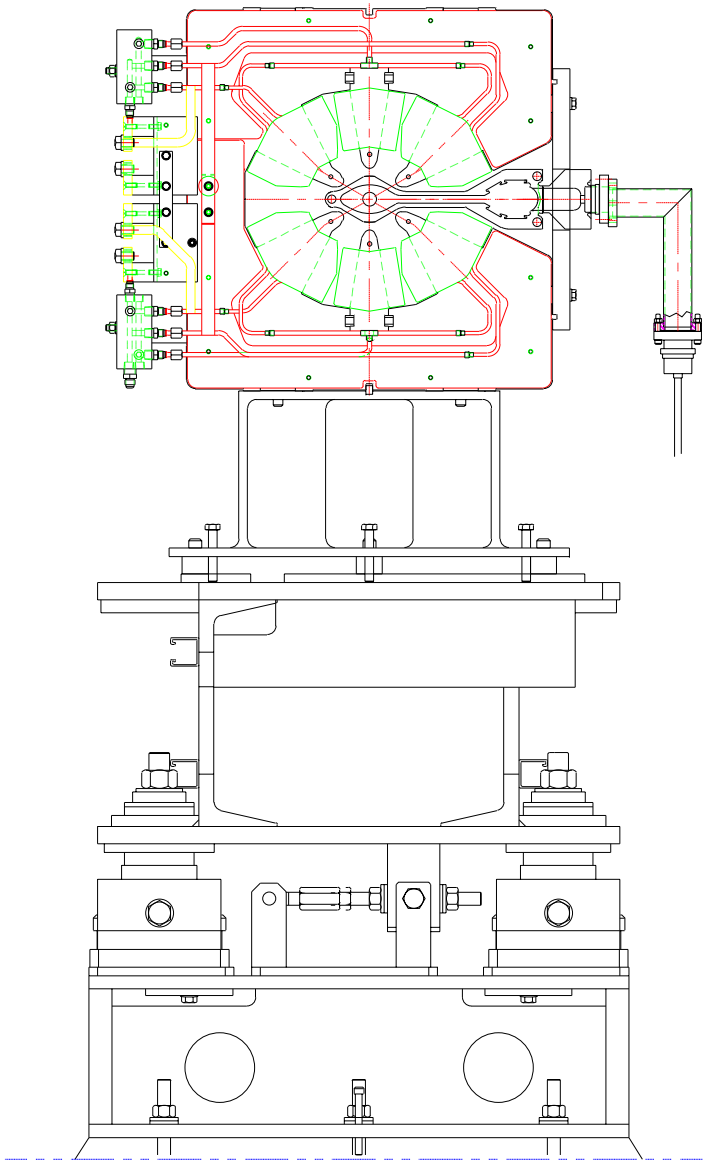

A Girder - Side View

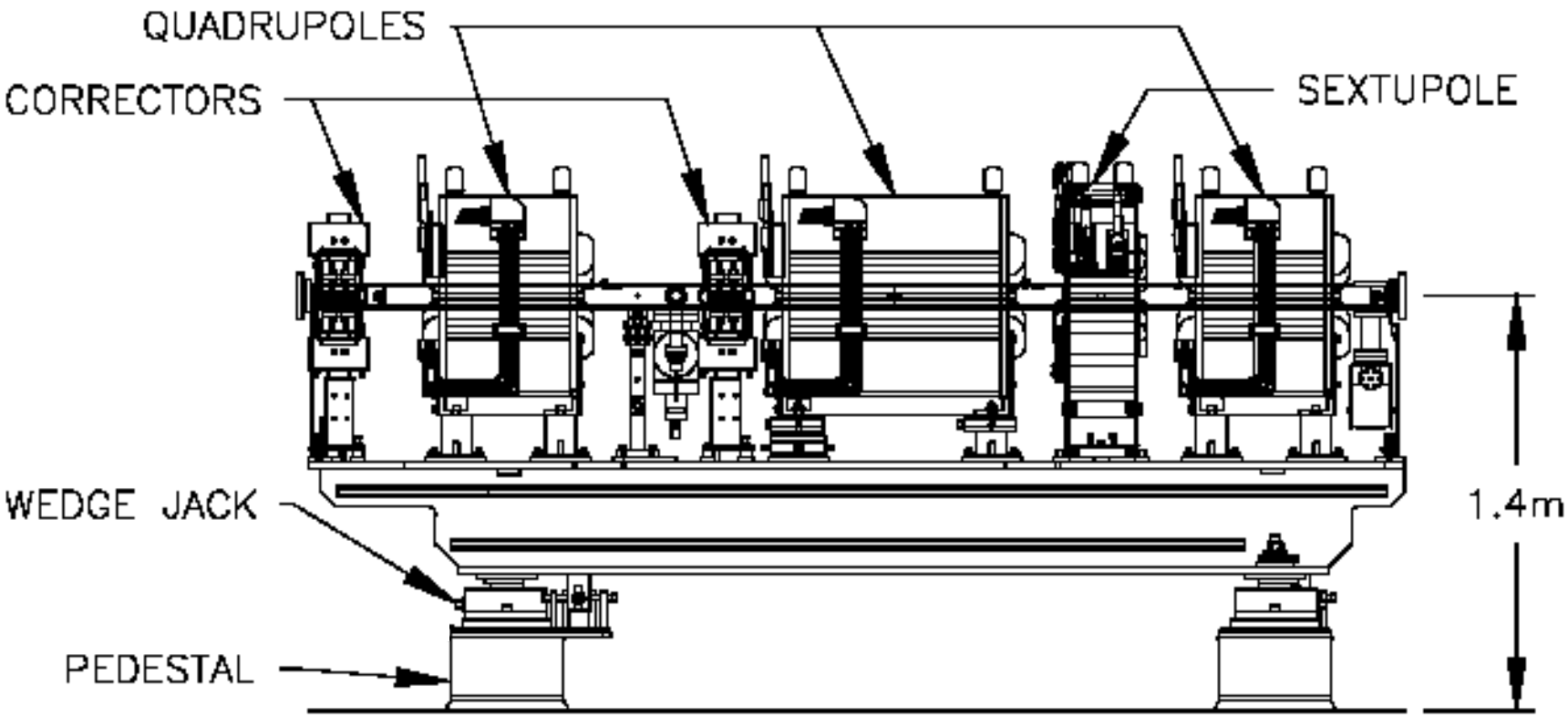

A Girder Resonance

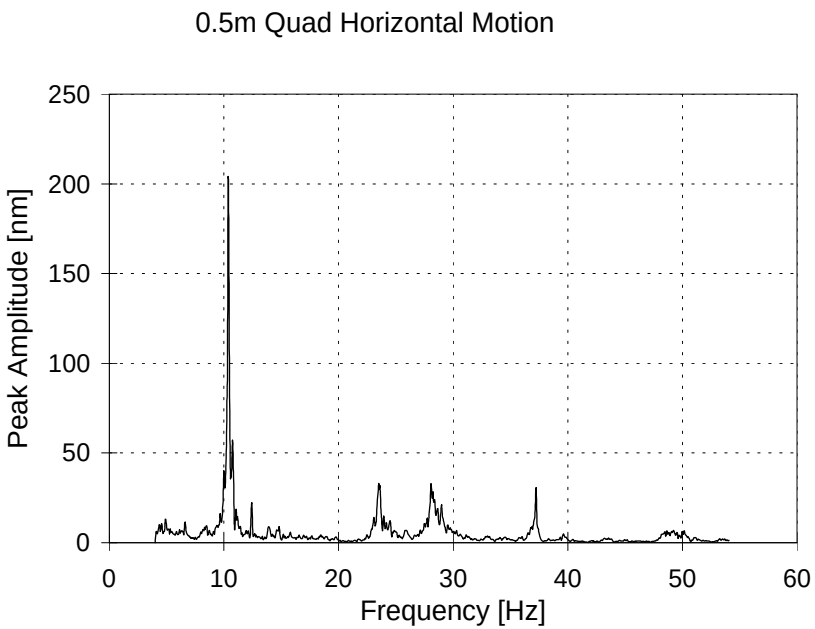

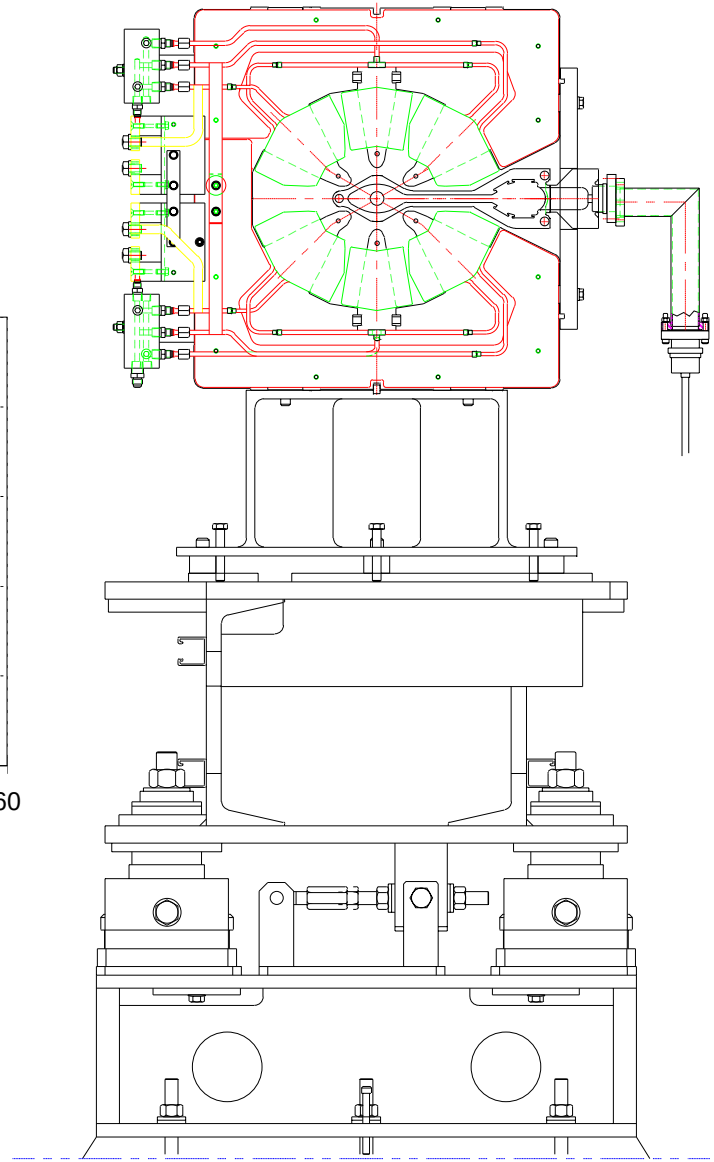

G. Decker etal http://accelconf.web.cern.ch/accelconf/p95/ARTICLES/FAR/FAR19.PDF

Test Pedestal / Magnet Assembly

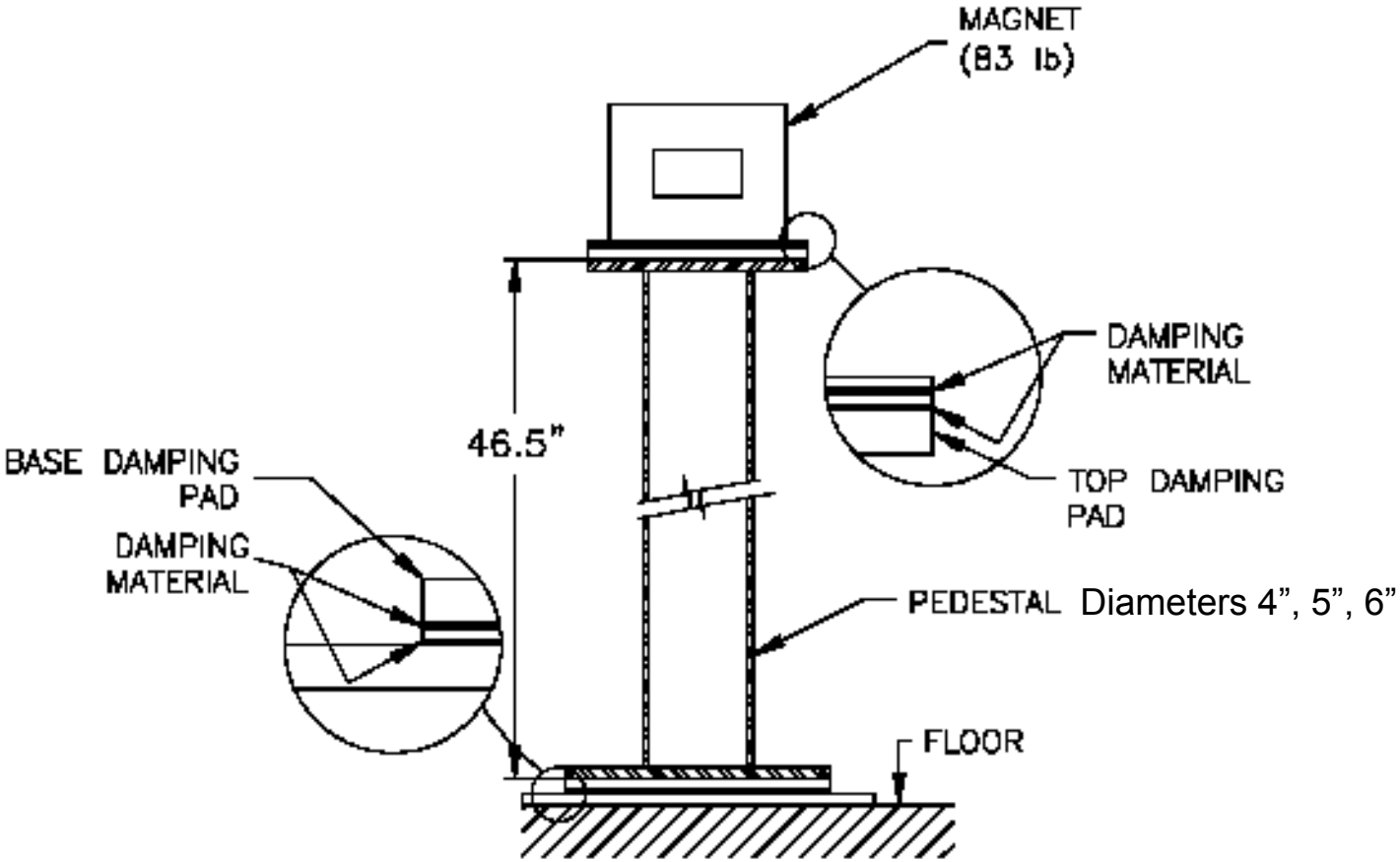

S. Sharma MEDSI 2000
http://www.aps.anl.gov/asd/me/Public/Papers(pdf)/vibration.pdf

Typical Ground Motion Spectrum

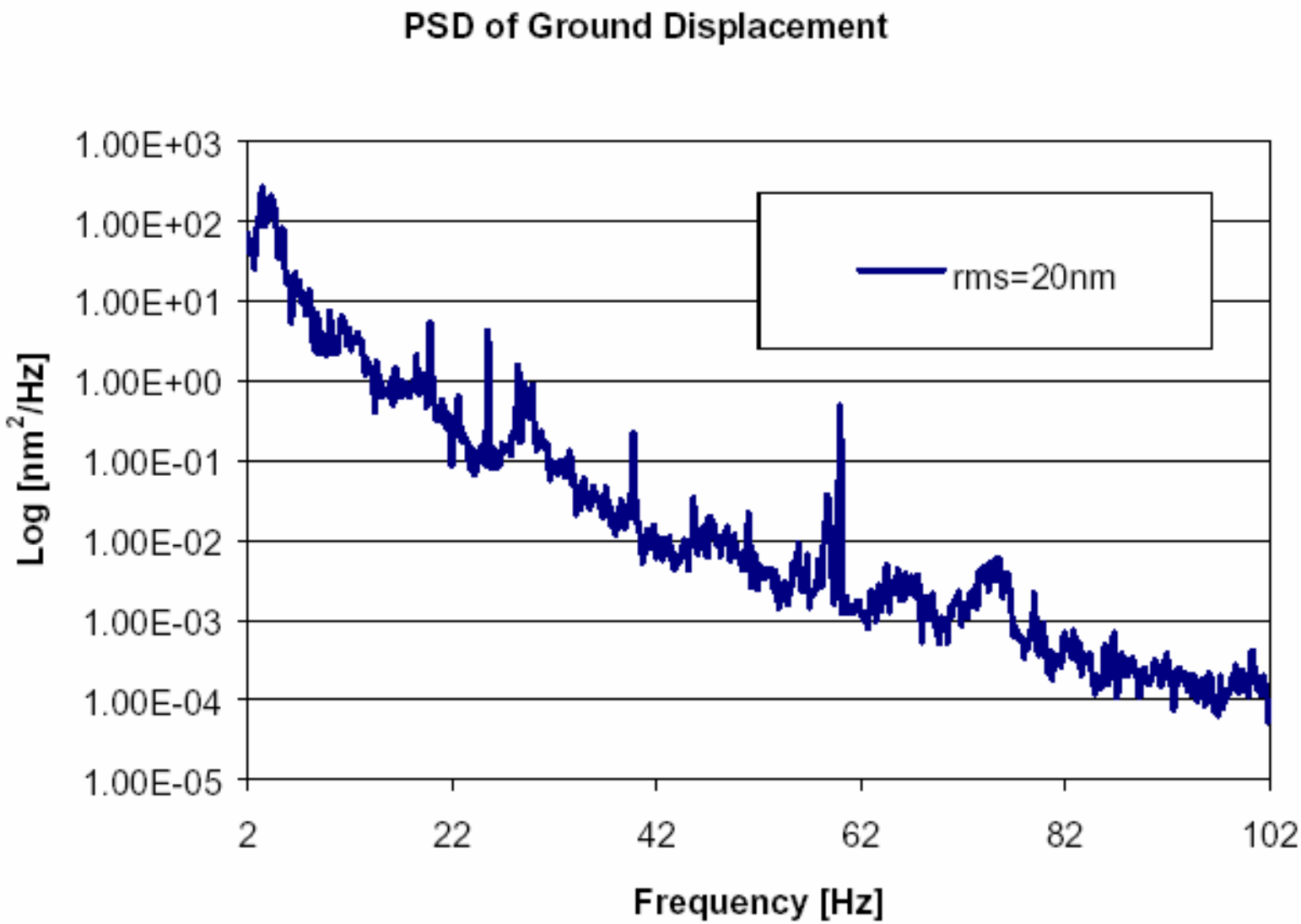

S. Sharma MEDSI 2000
http://www.aps.anl.gov/asd/me/Public/Papers(pdf)/vibration.pdf

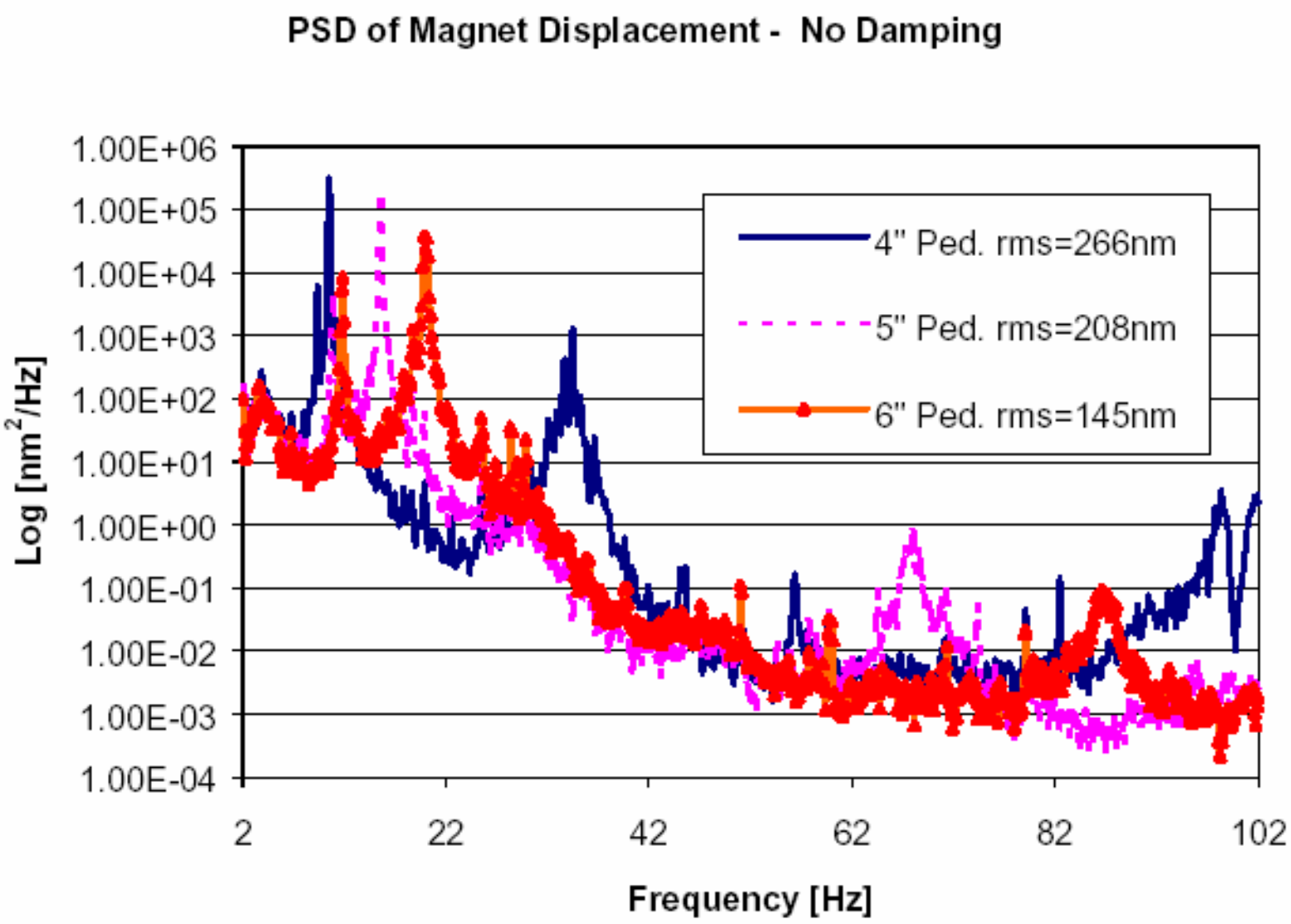

S. Sharma MEDSI 2000
http://www.aps.anl.gov/asd/me/Public/Papers(pdf)/vibration.pdf

Laminated Damping Pad

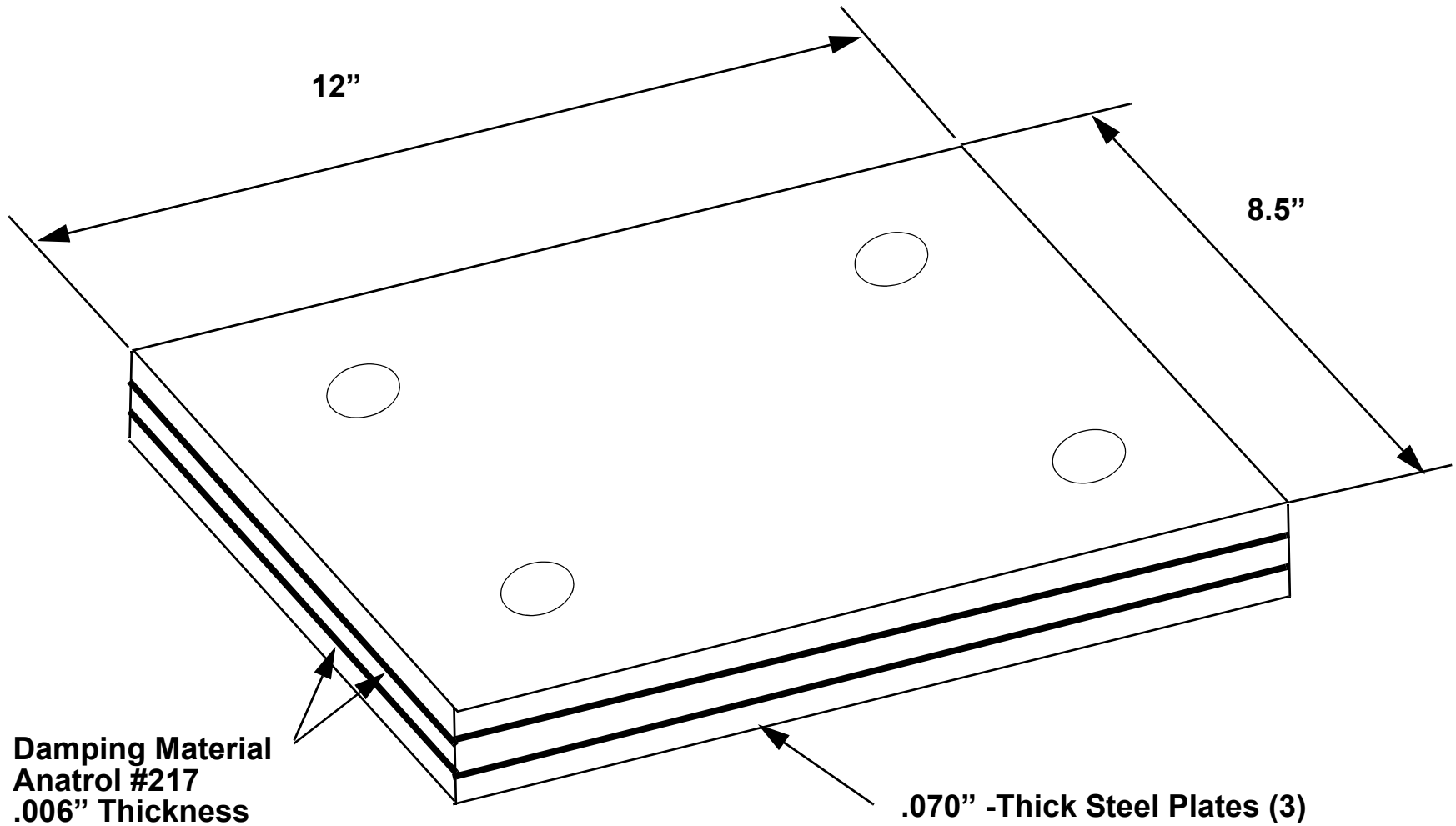

Visco-elastic Material Properties

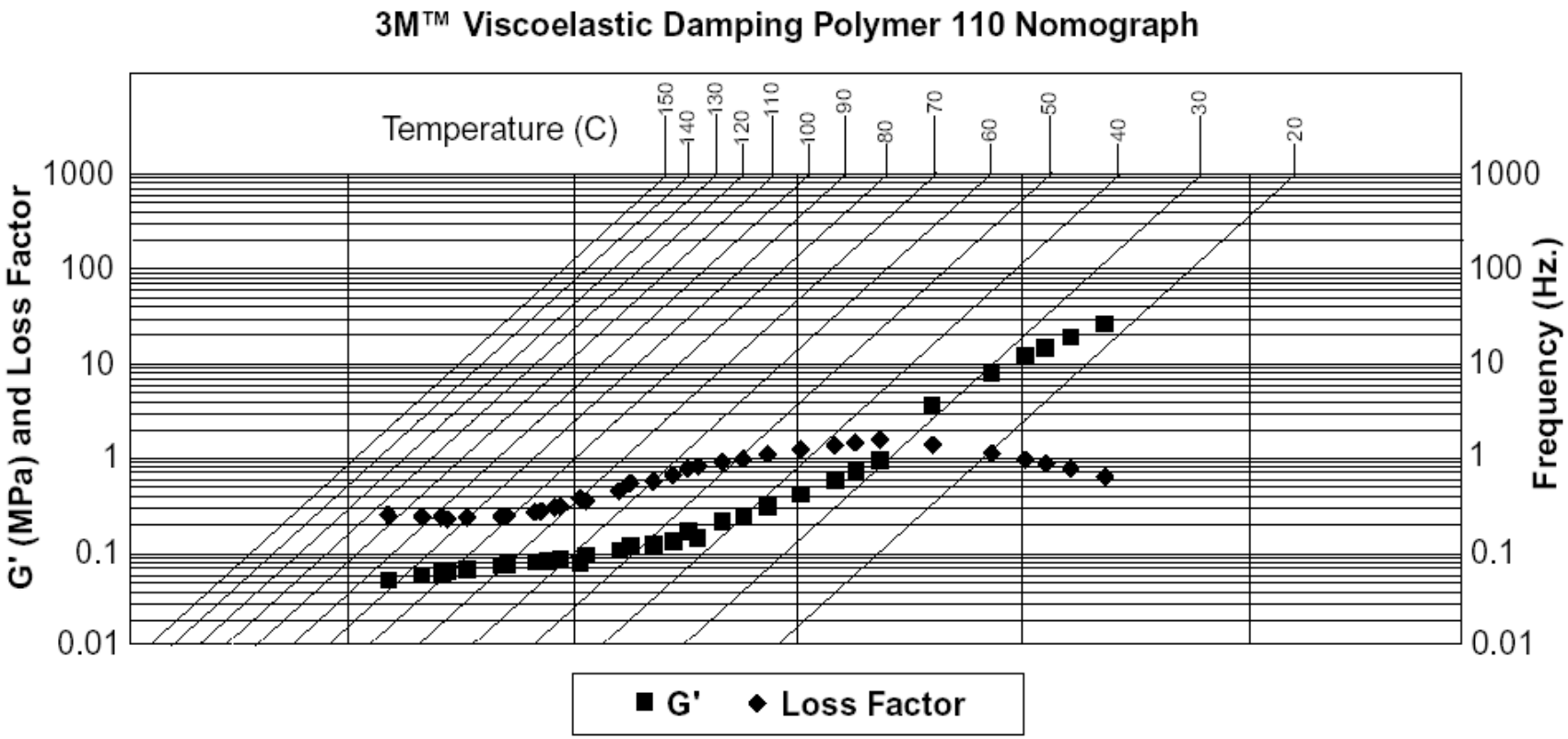

http://multimedia.mmm.com/mws/mediawebserver.dyn?WWWWWWWECOgjWpzXWizXWWWbEkGqUmxHb-

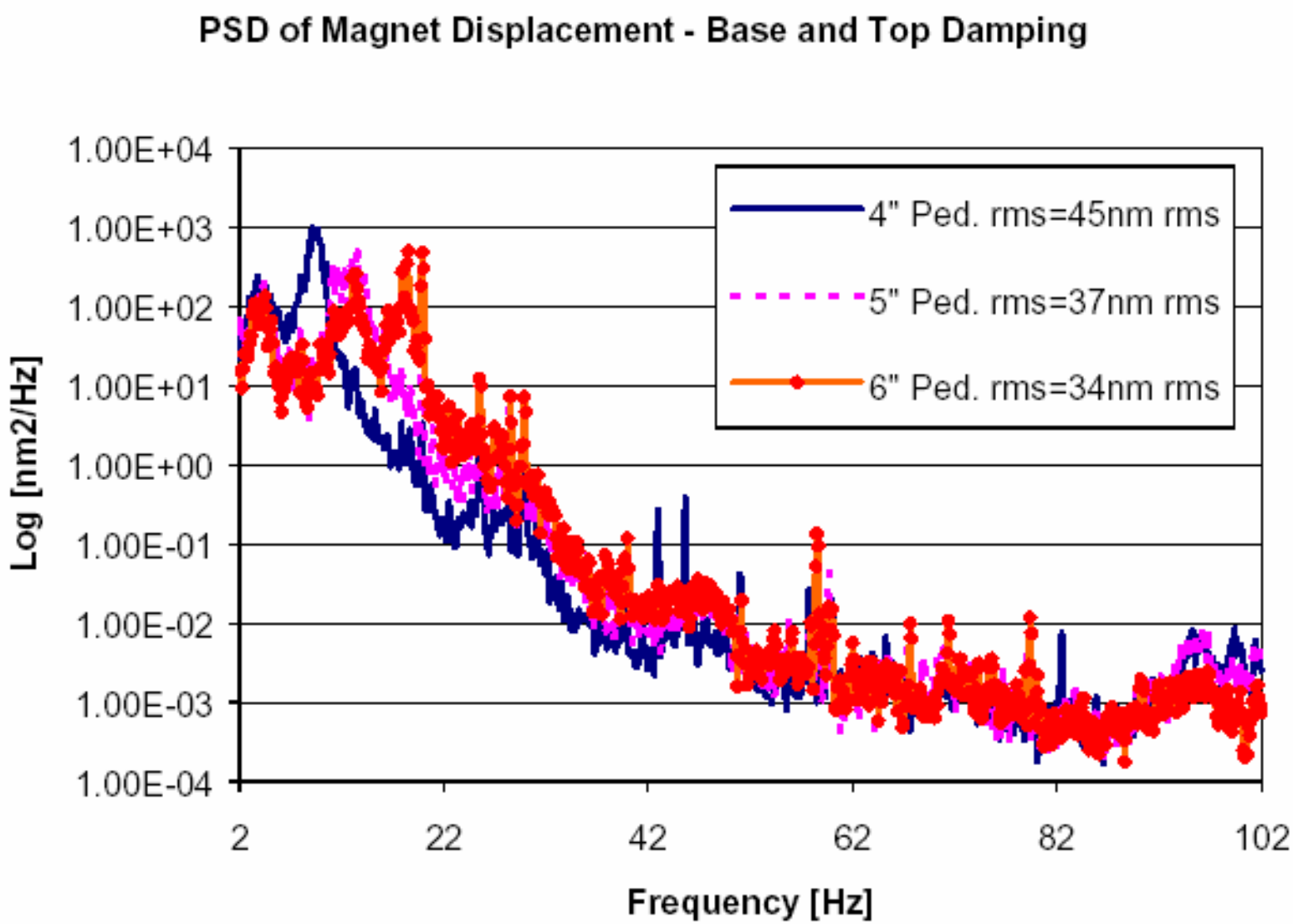
PSD of Magnet Displacement - Base and Top Damping
1.00E+04
1.00E+03
1.00E+02
1.00E+01
1.00E+00
1.00E-01
1.00E-02
1.00E-03
1.00E-04
Log [nm2/Hz]
2
22
42
62
82
102
Frequency [Hz]
4" Ped. rms=45nm rms
5" Ped. rms=37nm rms
6" Ped. rms=34nm rms

Girder Transfer Function Measurement Arrangement

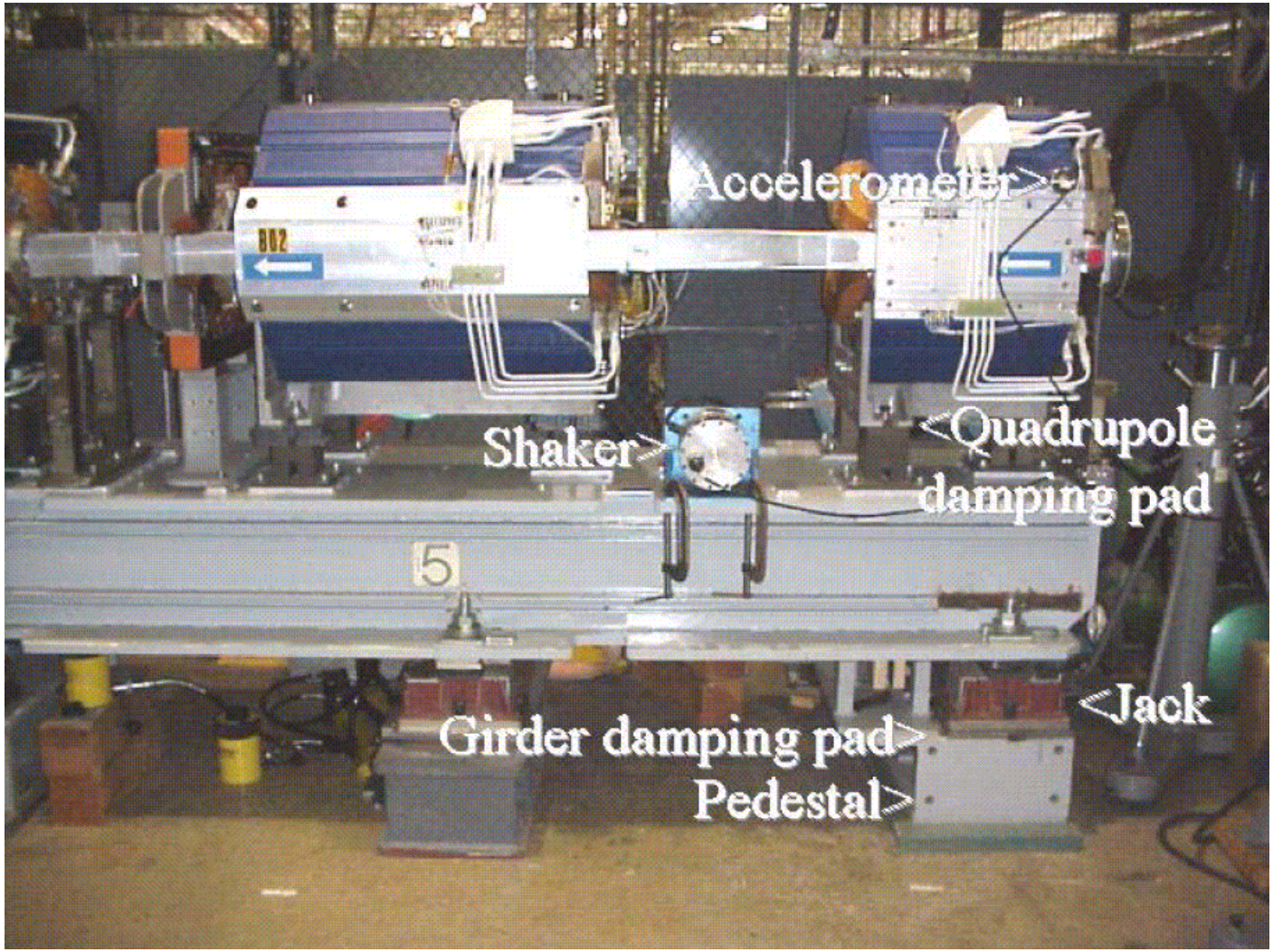

C. Doose, S. Sharma, MEDSI'02,
http://www.aps.anl.gov/asd/me/medsi02/papers/MED021.pdf

Case 1 Swept-Sine Measurement Transfer Functions

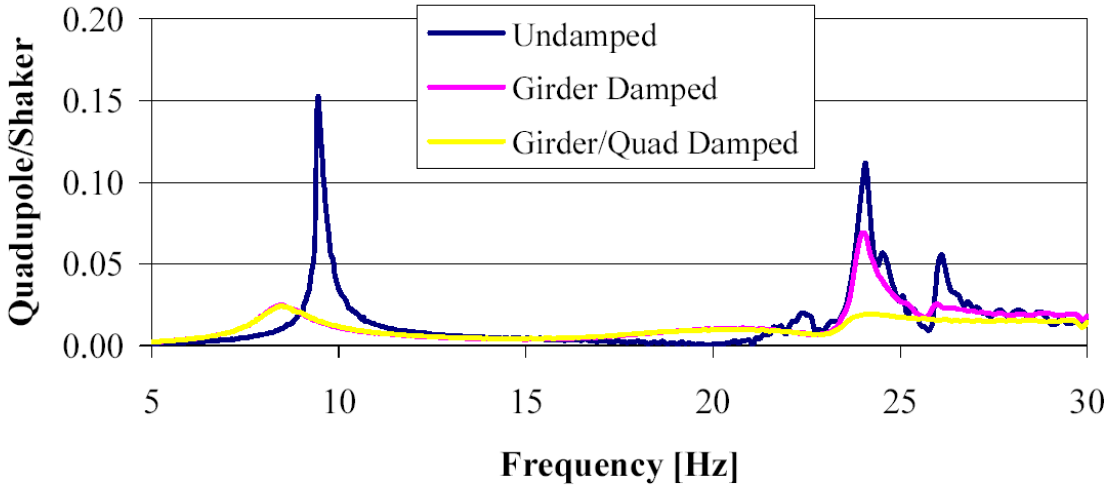

Case1 FFT Measurement Transfer Functions

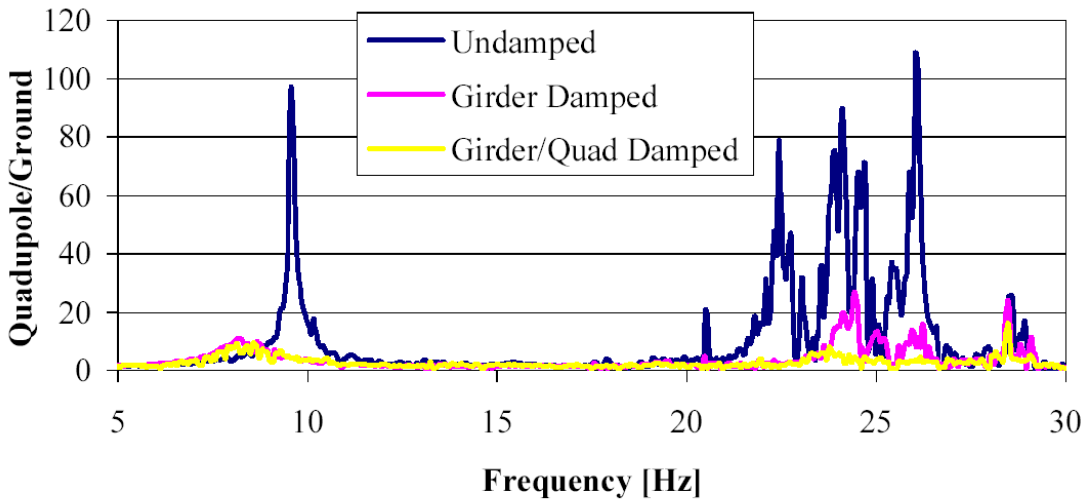

C. Doose, S. Sharma, MEDSI'02,
http://www.aps.anl.gov/asd/me/medsi02/papers/MED021.pdf

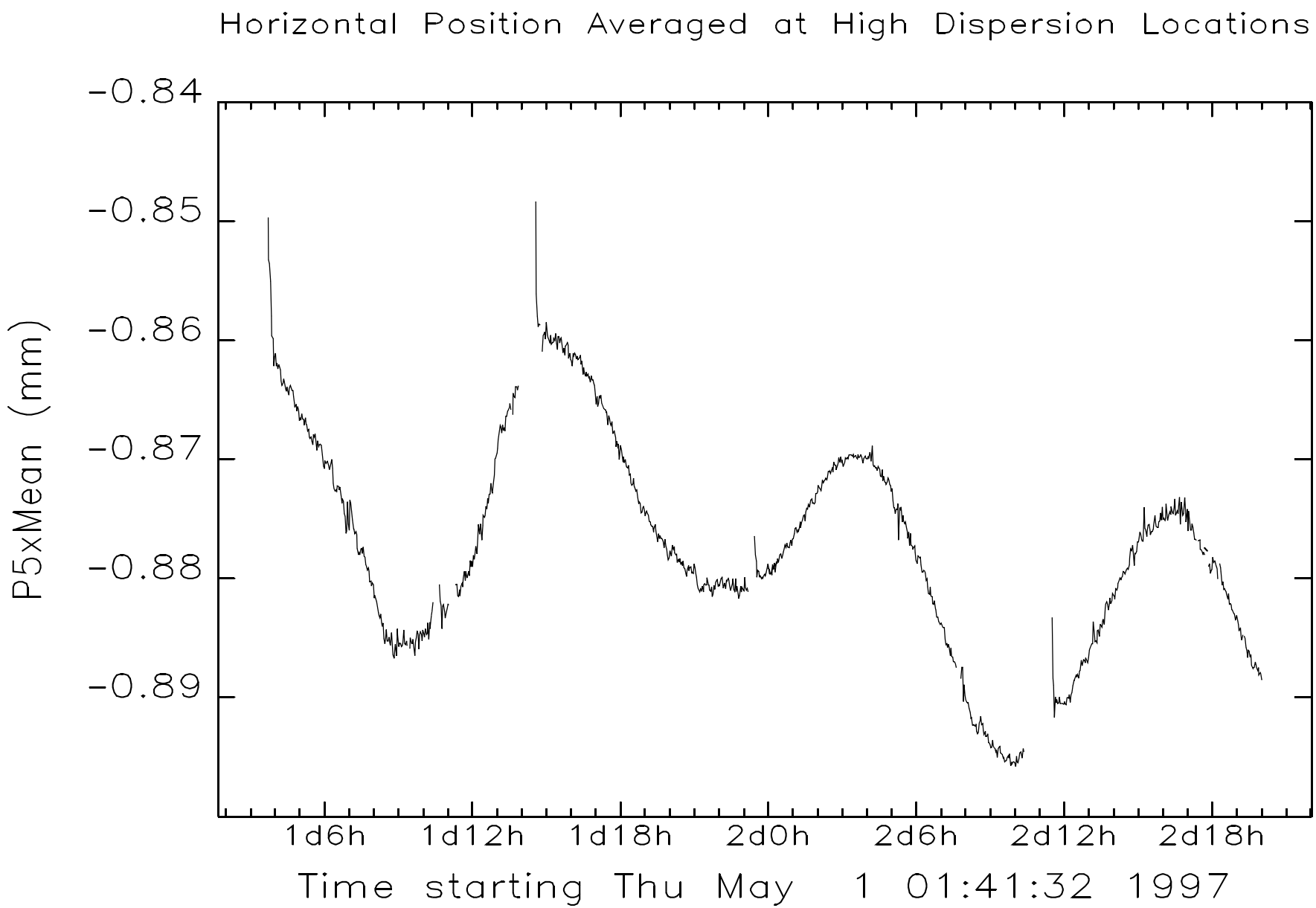
Horizontal Position Averaged at High Dispersion Locations
-0.84
-0.85
-0.86
-0.87
-0.88
-0.89
P5xMean (mm)
1d6h
1d12h
1d18h
2d0h
2d6h
2d12h
2d18h
Time starting Thu May 1 01:41:32 1997

Gravity Fluctuations Showing Beating between Solar and Lunar Tides

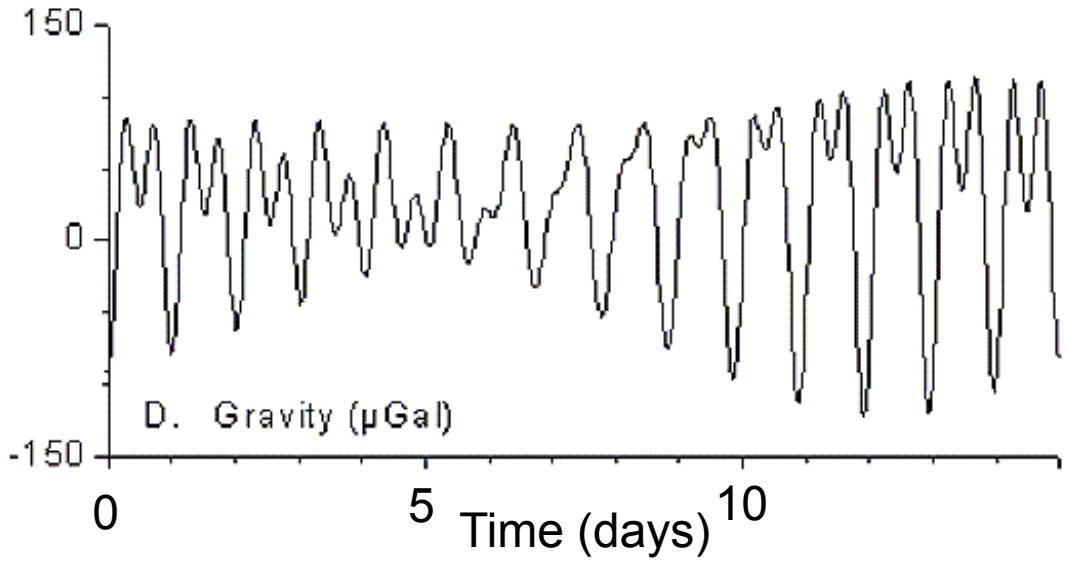

K1, O1, S2, and M2 respectively represent the luni-solar diurnal, principal lunar diurnal, principal solar semi-diurnal, and principal lunar semi-diurnal components.

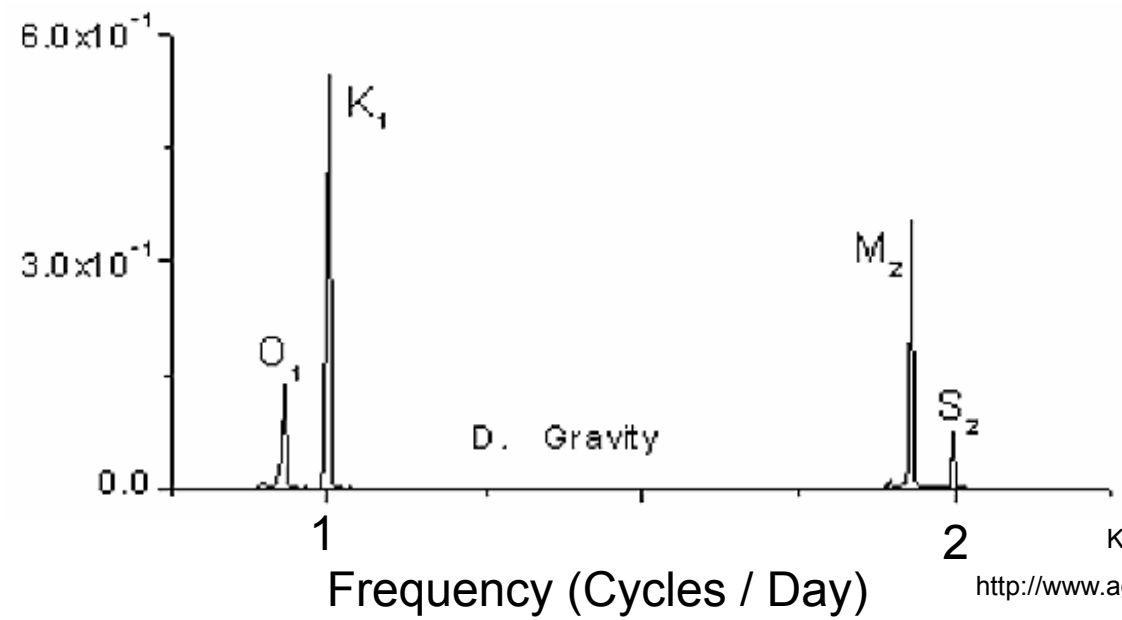

Kulessa, B, etal, Geophys. Res. Lett.,30(1), 1011, (2003)

http://www.agu.org/pubs/sample_articles/cr/2002GL015303/5.shtml

Measured deviation of APS storage ring circumference from 1104 meter design value for operational period 98-1

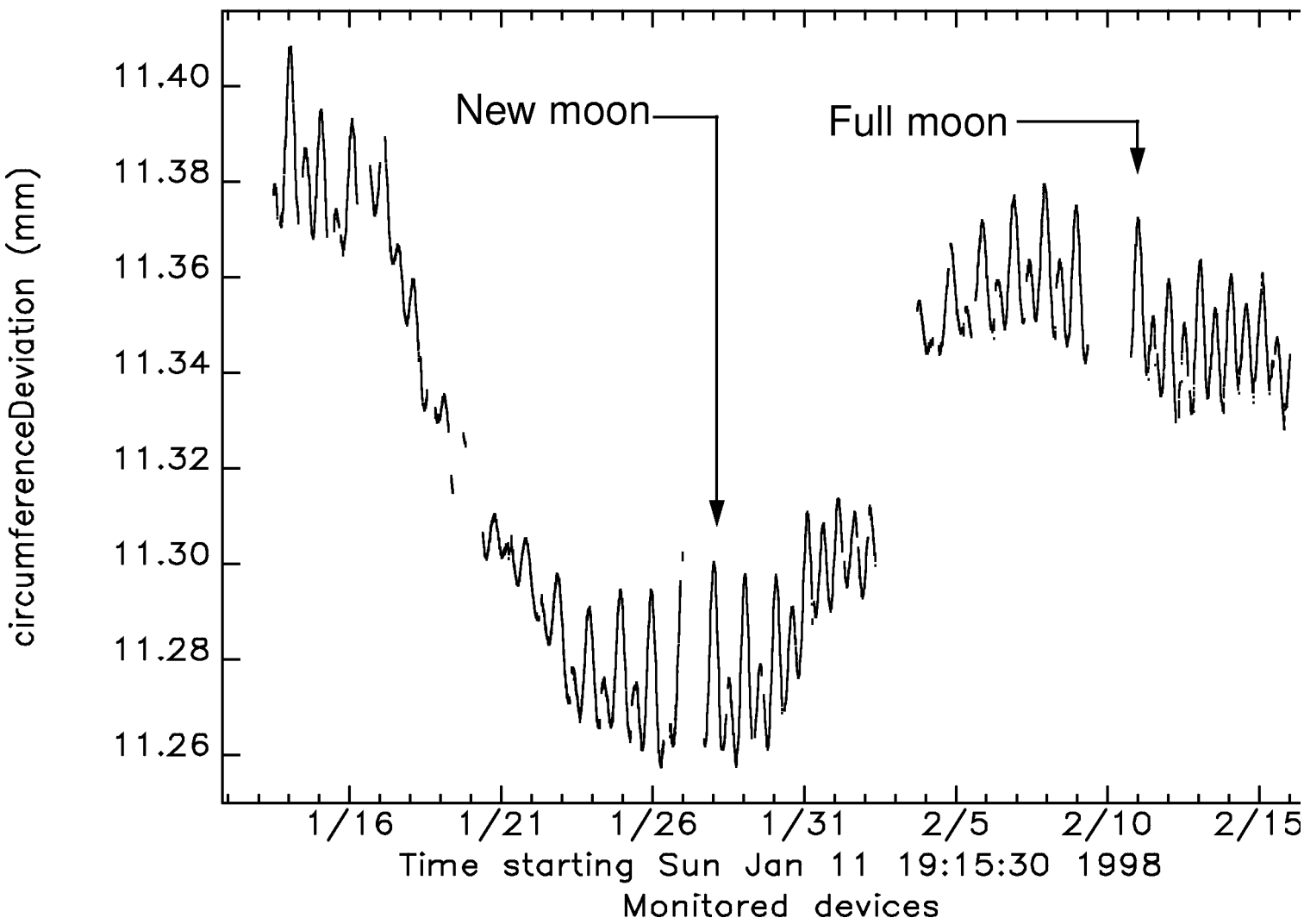

Fourier transform of measured deviation of APS storage ring circumference from 1104 meter design value for operational period 98-1

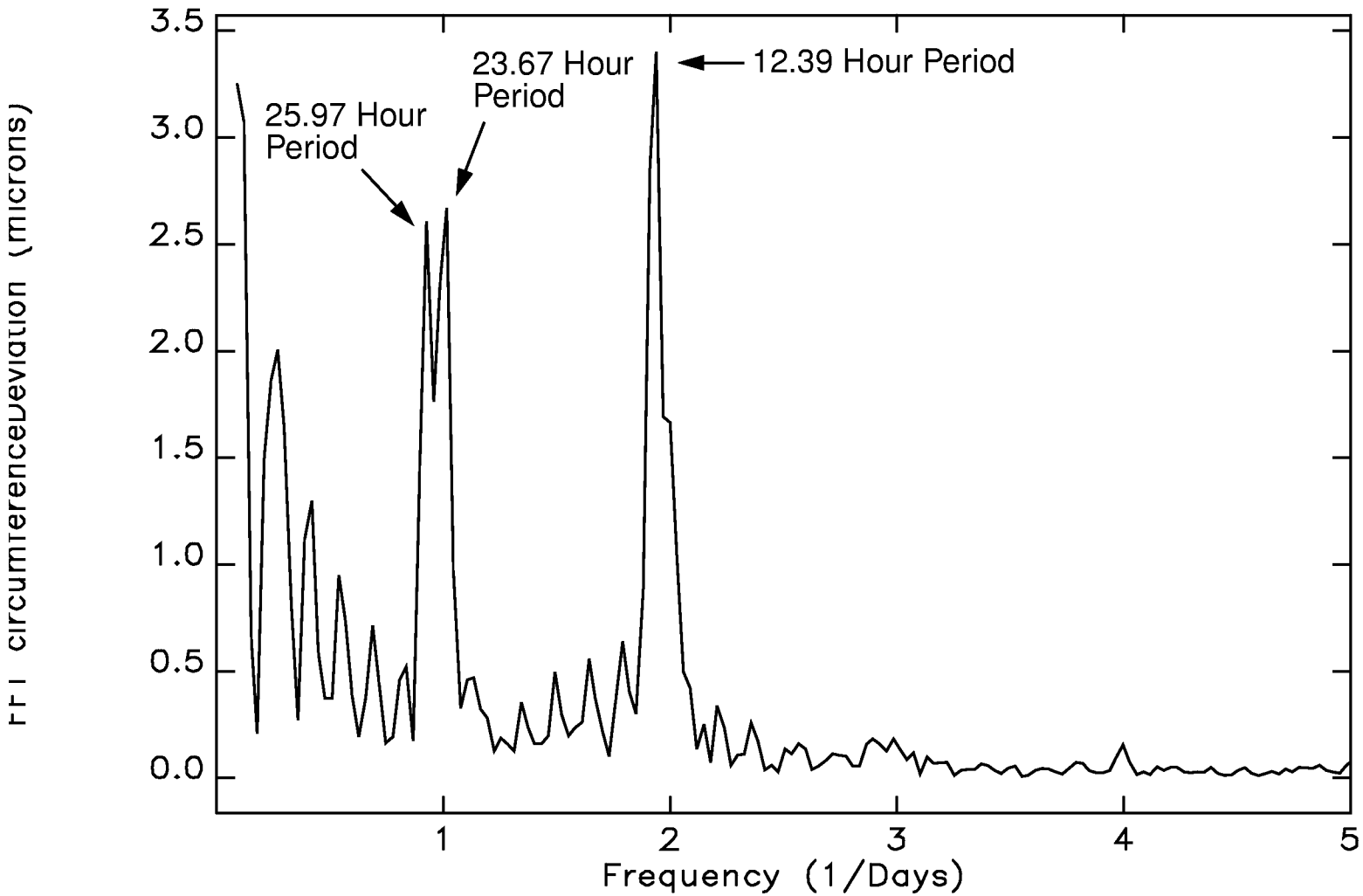

Sources of Beam Instability

- Electromagnetic

-Power Supplies

- Insertion Devices

-RF

Sources of Beam Instability - Magnetic Field Errors

A localized change in transverse magnetic field $\delta B(s)$ will introduce a kick

$$\Delta x' = \frac{1}{B\rho}\int \delta B(s)\,ds$$

which in turn will cause a closed orbit distortion with a kink in it:

$$\Delta x(s) = \frac{\sqrt{\beta_x(s)\beta_1}\,\Delta x_1'}{2\sin\pi\nu_x}\cos[\psi_x(s) - \psi_x(s_1) + \nu_x\pi] \quad s < s_1$$

$$= \frac{\sqrt{\beta_x(s)\beta_1}\,\Delta x_1'}{2\sin\pi\nu_x}\cos[\psi_x(s_1) - \psi_x(s) + \nu_x\pi] \quad s > s_1$$

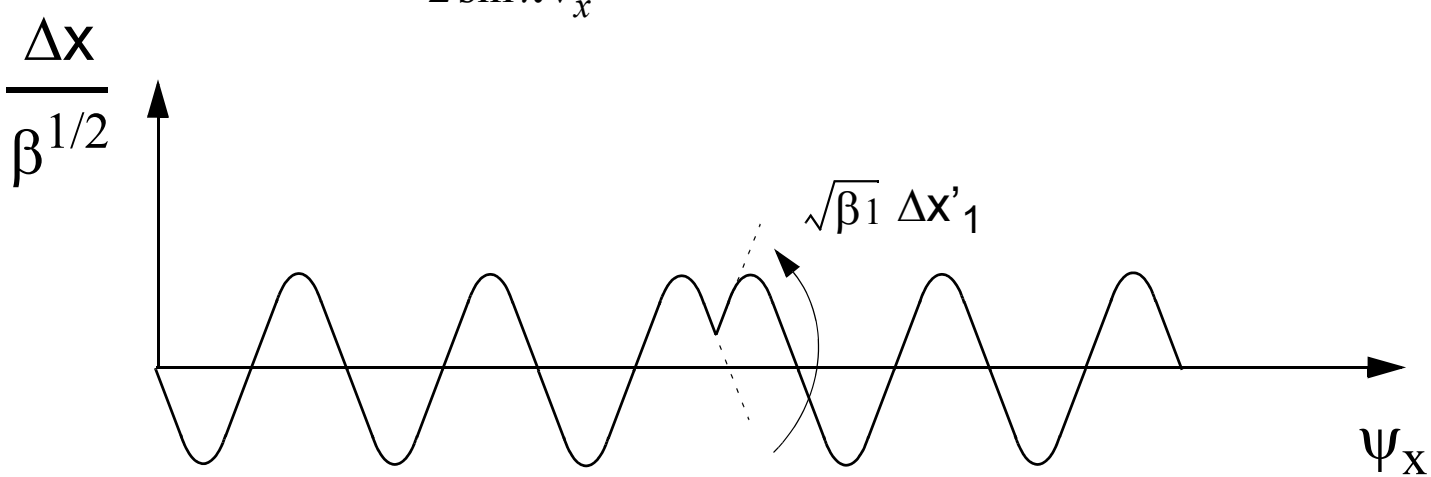

Steering Correctors as Sources of Beam Instability

The APS uses pulse-width-modulation power supplies to control the orbit, a total of 317 in each of x, y

The steering corrector magnets are combined-function horizontal / vertical correctors. Each magnet has two associated power supplies.

Of the 317 magnets, 38 are "high speed" correctors, the so-called "AV3" magnets. This allows orbit control at frequencies up to approx. 100 Hz. The balance are "slow" correctors, with only a few Hz bandwidth.

Note - the vertical beta function is large (> 20 meters) at the AP4 bpm locations.

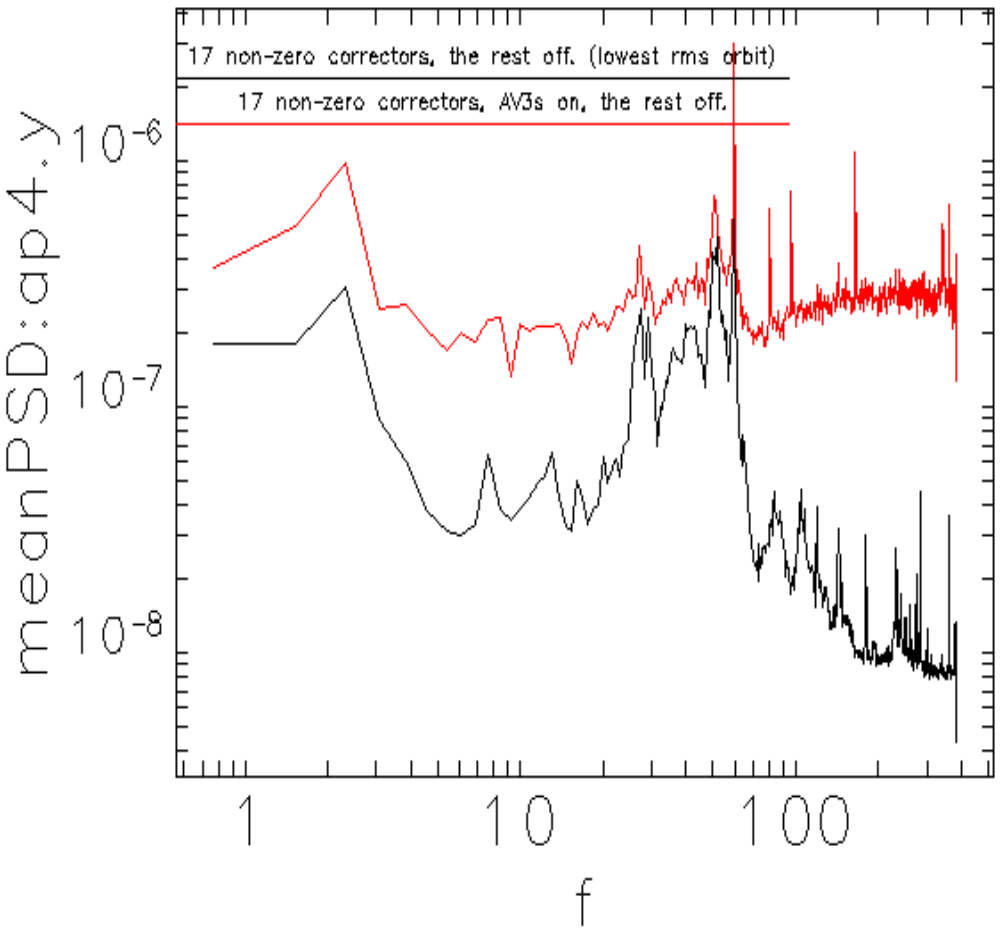

Data Courtesy of L. Emery, APS

Effect of fast correctors, in sensible units

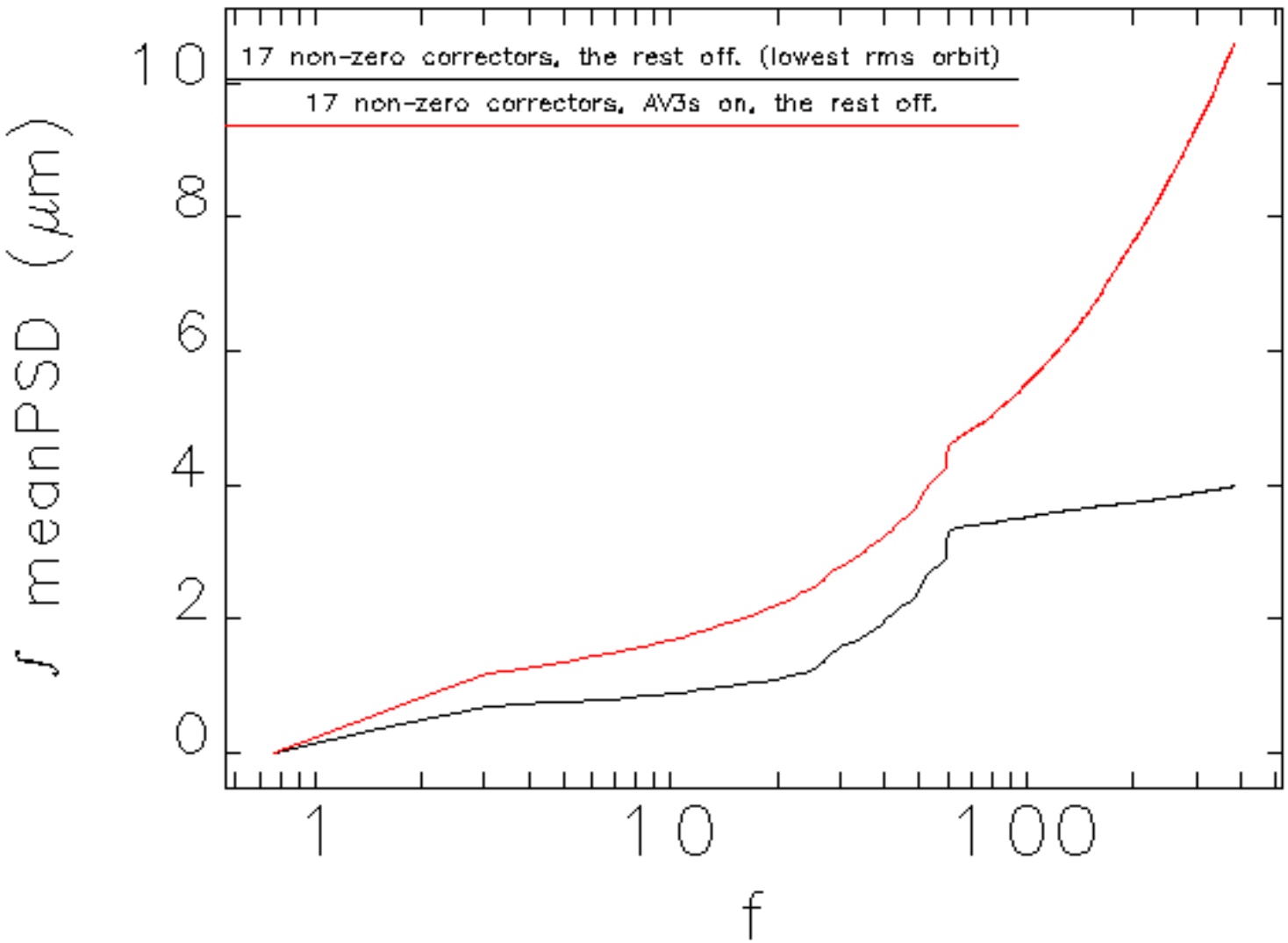

Data Courtesy of L. Emery, APS

All except fast correctors on, most at zero setpoint

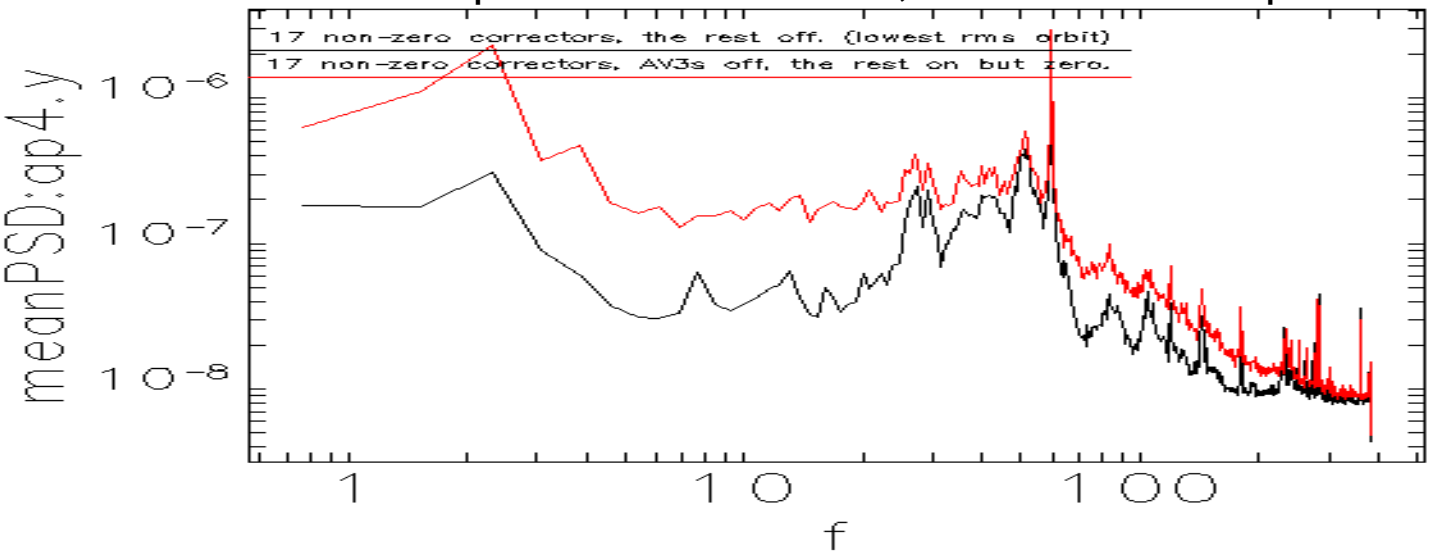

Only fast correctors plus minimal number of slow correctors on.

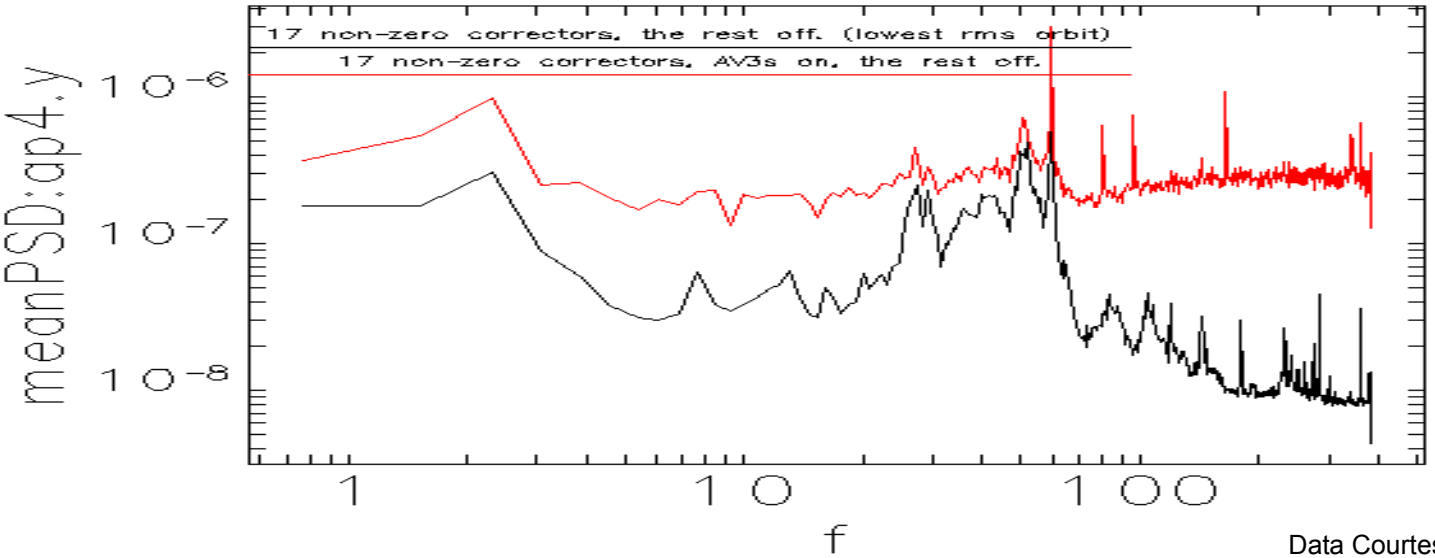

Data Courtesy of L. Emery, APS

All except fast correctors on, most at zero setpoint

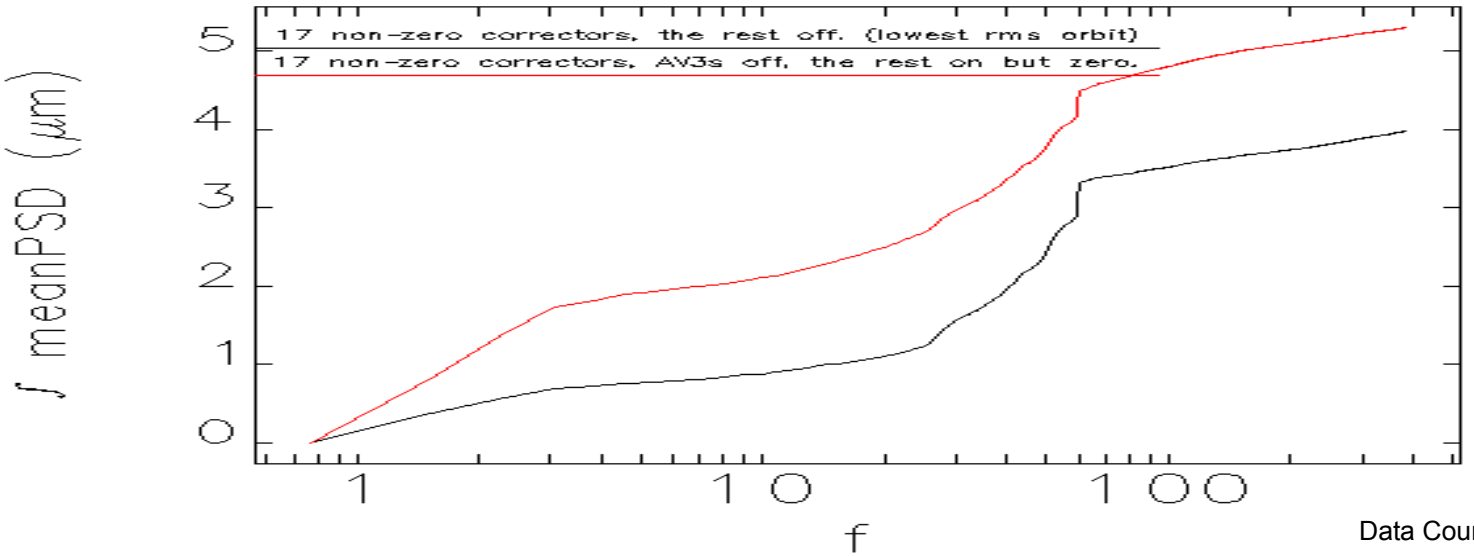

Data Courtesy of L. Emery, APS

Only fast correctors plus minimal number of slow correctors on.

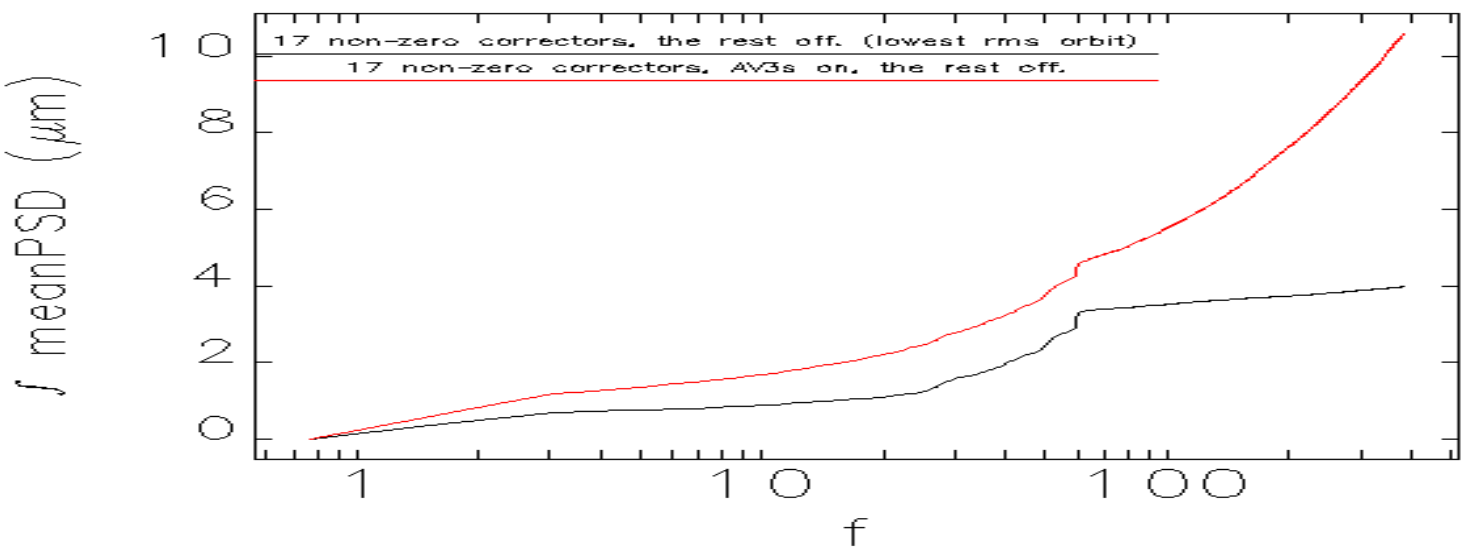

Typical Integrated Noise at BPM's Near Insertion Device Source Points

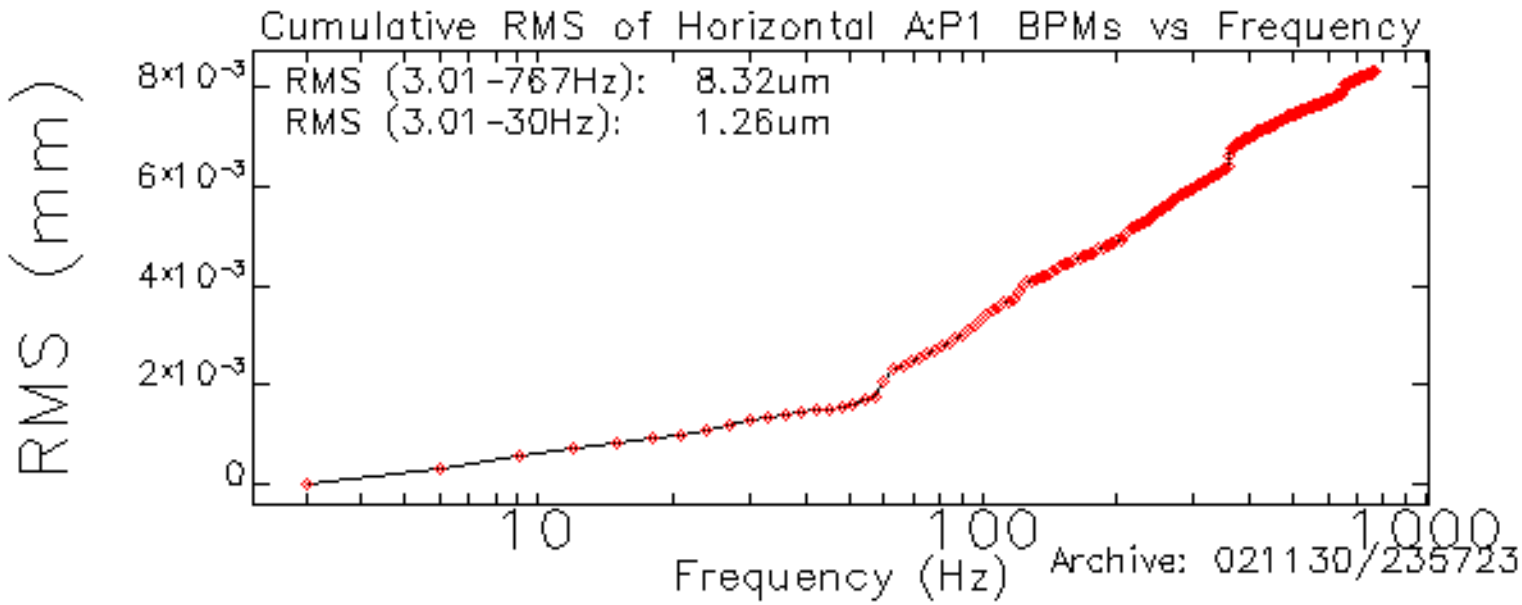

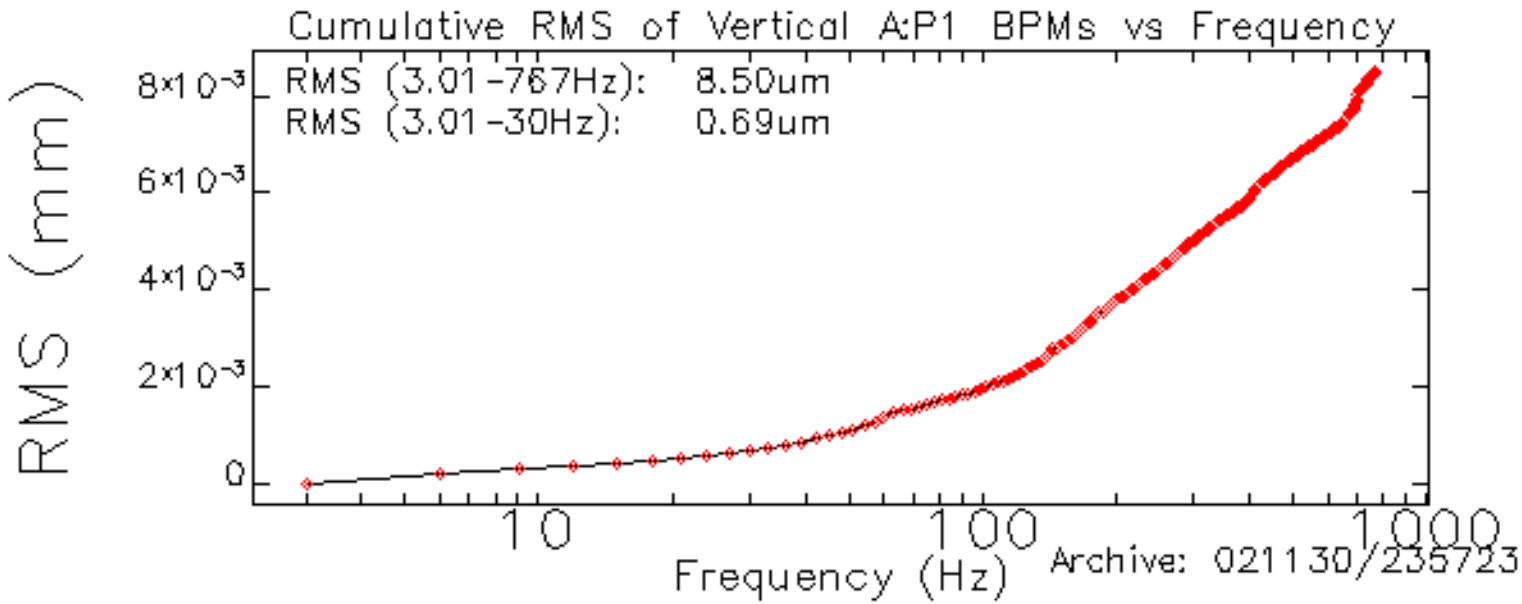

Data Courtesy of L. Emery, APS

Beam Motion RMS

Real-time calculation of RMS in three bands simultaneously

Three settable bands

RMS values

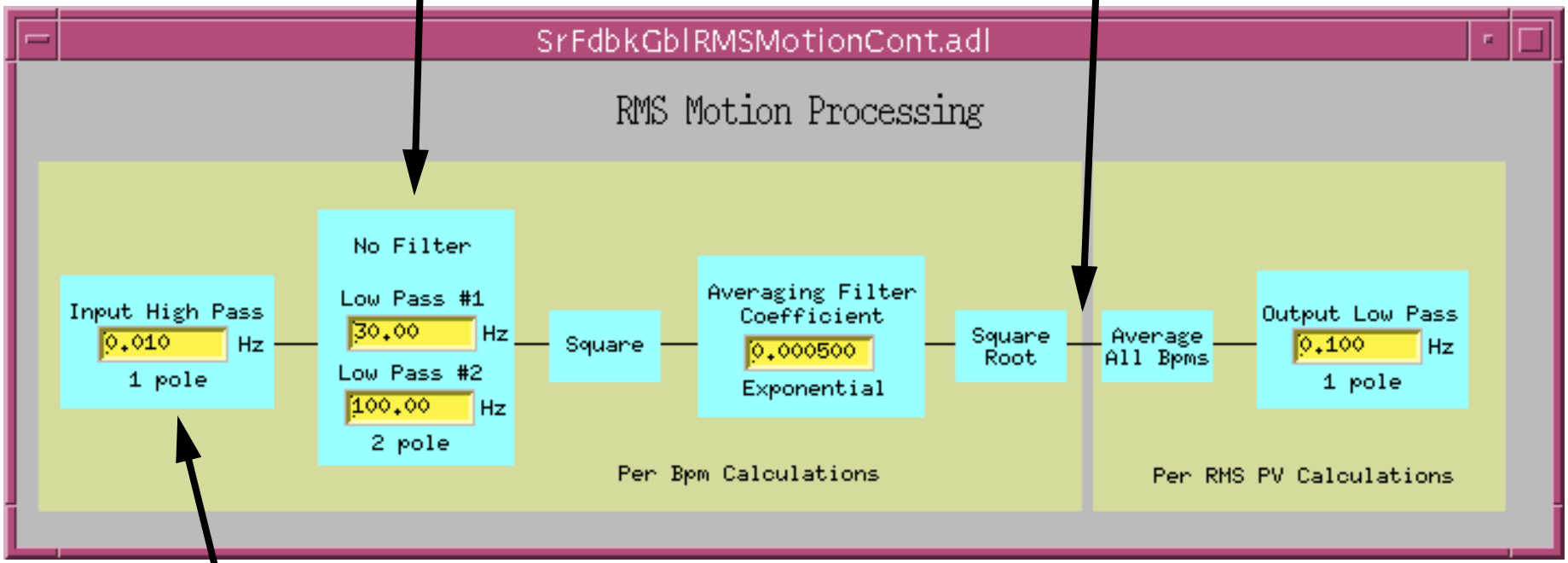

Data input
at sample rate

Graphic Courtesy of L. Emery, F. Lenkszus, APS

RMS Beam Stability Data

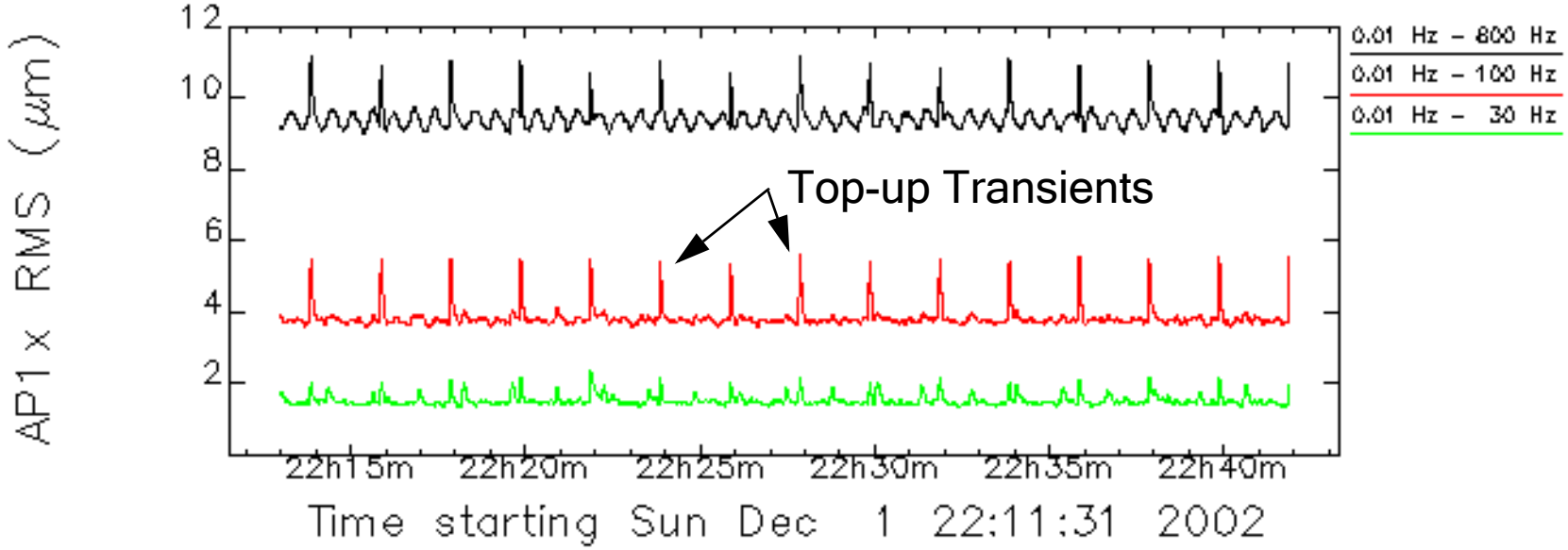

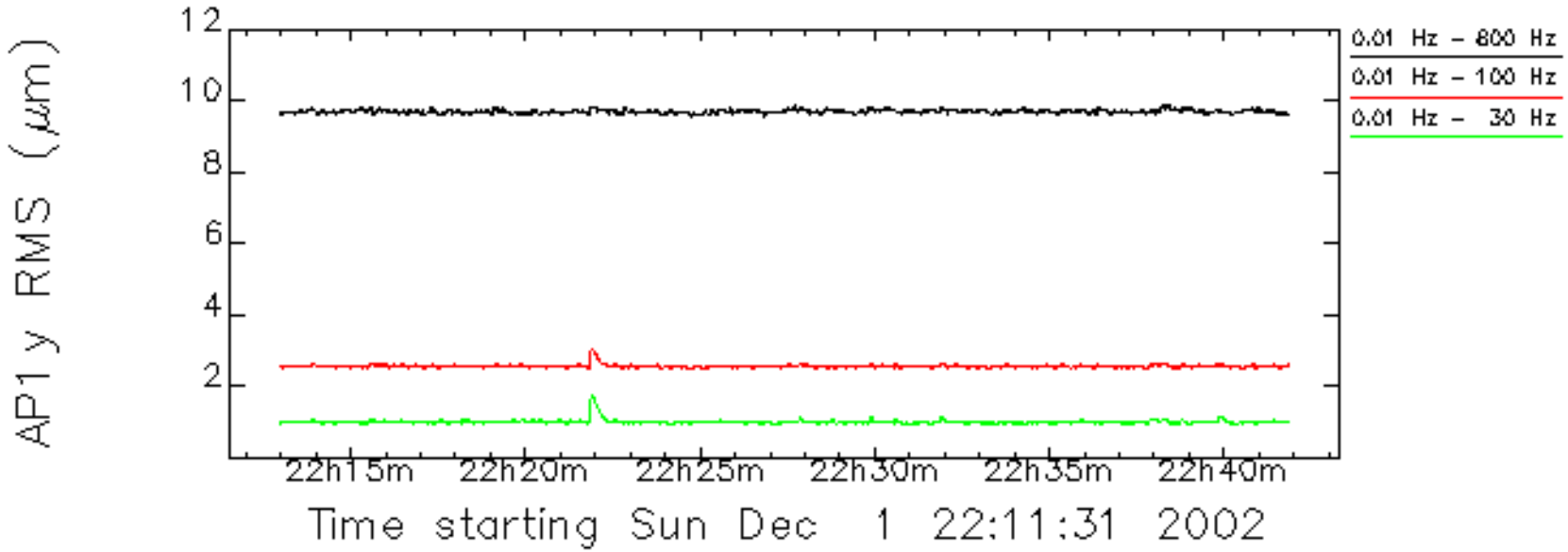

Data Courtesy of L. Emery, APS

Insertion Devices

Insertion device gaps are variable on demand by the users at the APS. Extremely strong variable magnetic fields result, especially at very small gaps. This results in

1) Steering error vs. gap

$$\Delta x' = \frac{1}{B\rho}\int B(s)\,\mathrm{d}s$$

Here the integral is along the entire length of the insertion device.

2) Step change in trajectory through the device:

$$\Delta x = \frac{1}{B\rho}\int\left(\int_s \delta B(s')\,\mathrm{d}s'\right)dS$$

3) Vertical focussing (even for a perfect device) -- impacts beam size

4) Energy loss - impacts emittance

Insertion Device Magnetic Measurement Data and Field Integrals

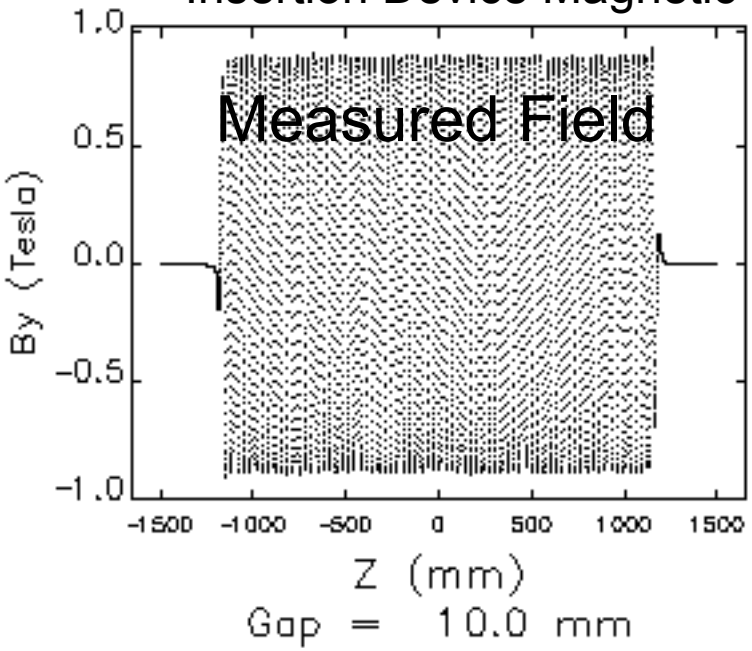

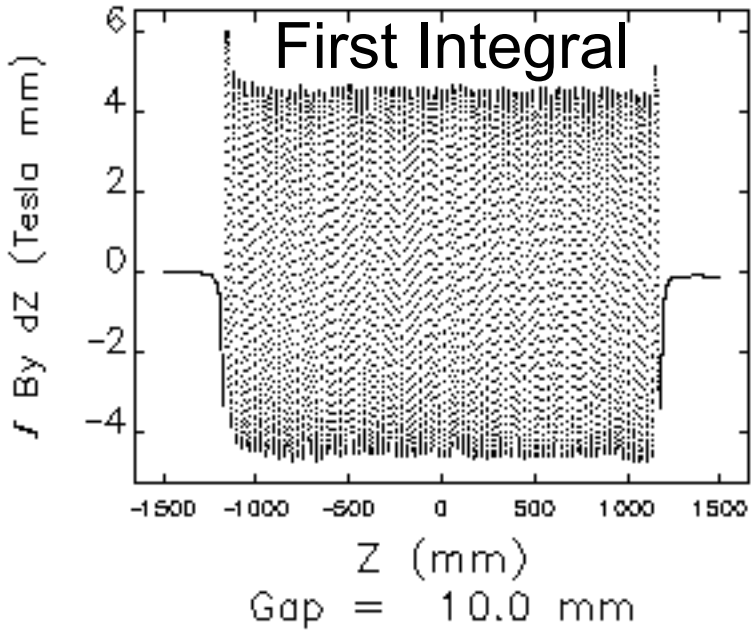

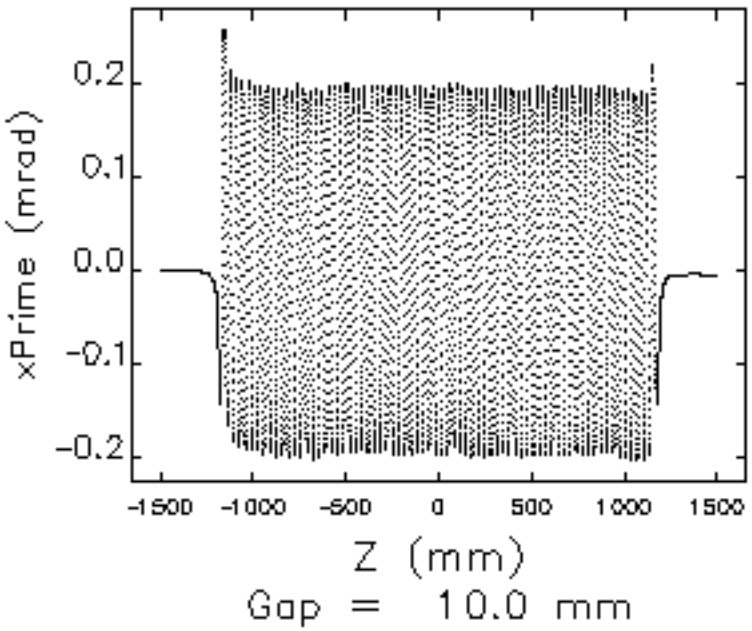

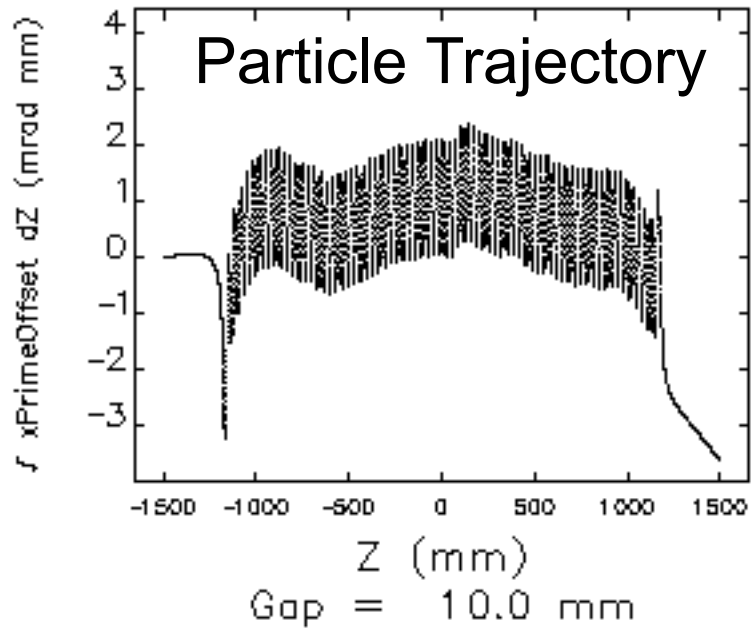

Insertion Device Magnetic Measurement Data and Field Integrals

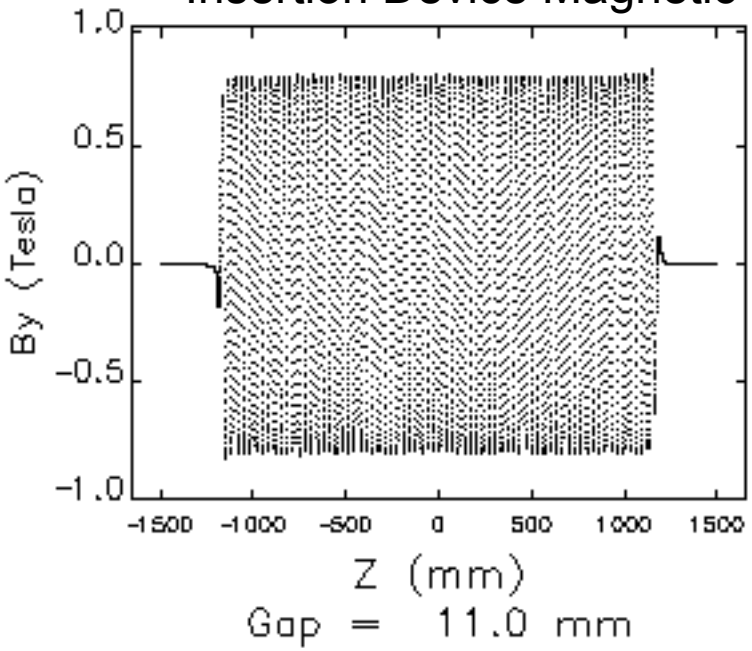

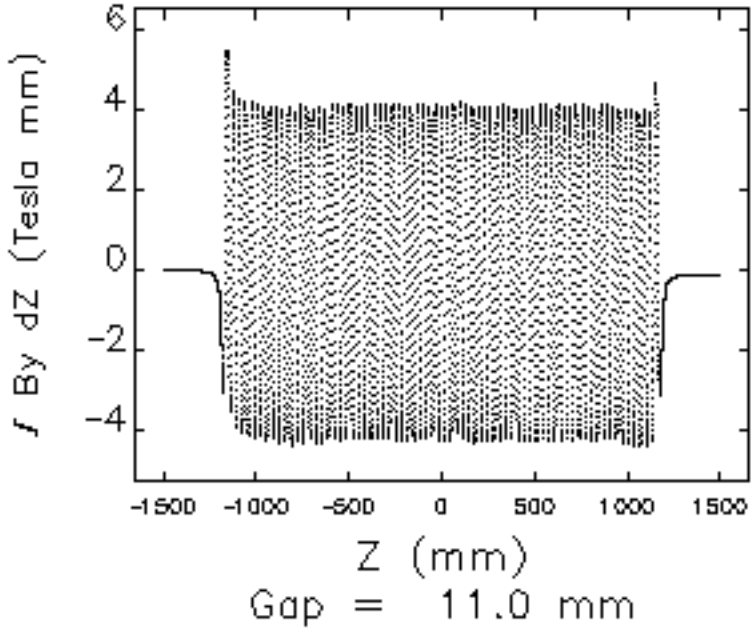

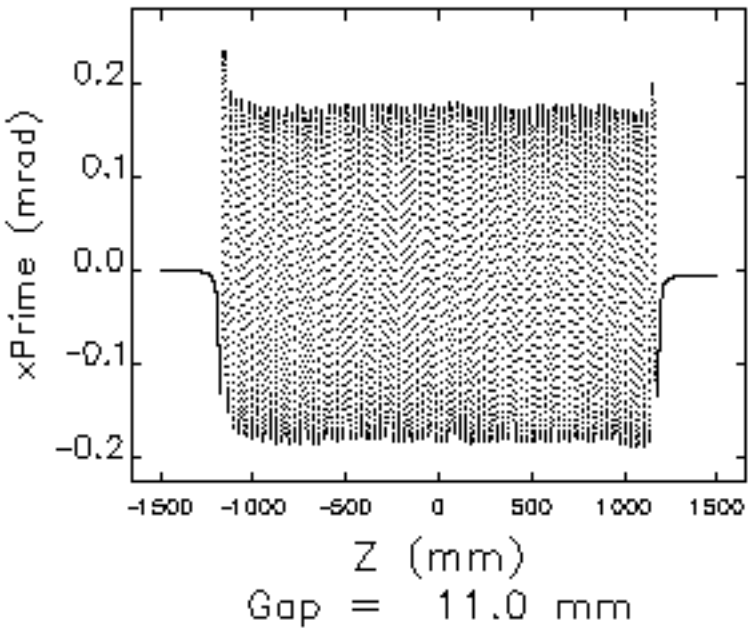

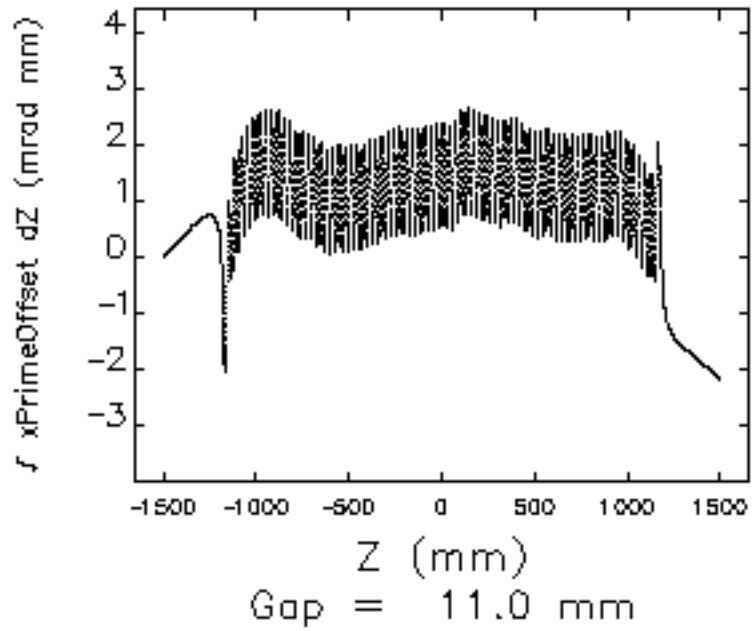

Insertion Device Magnetic Measurement Data and Field Integrals

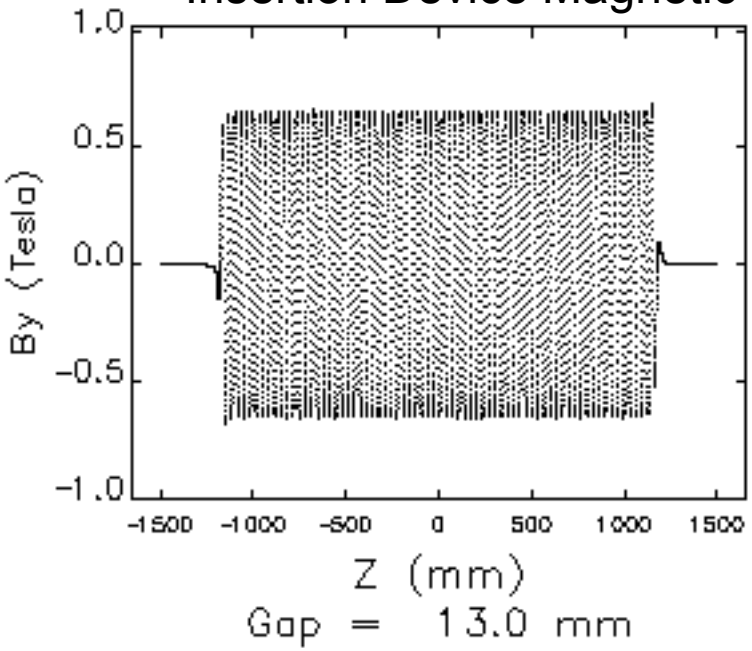

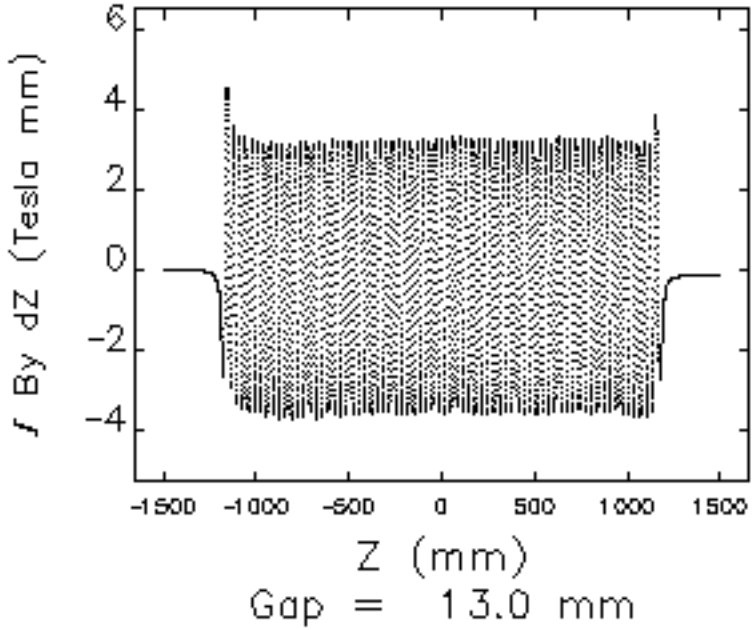

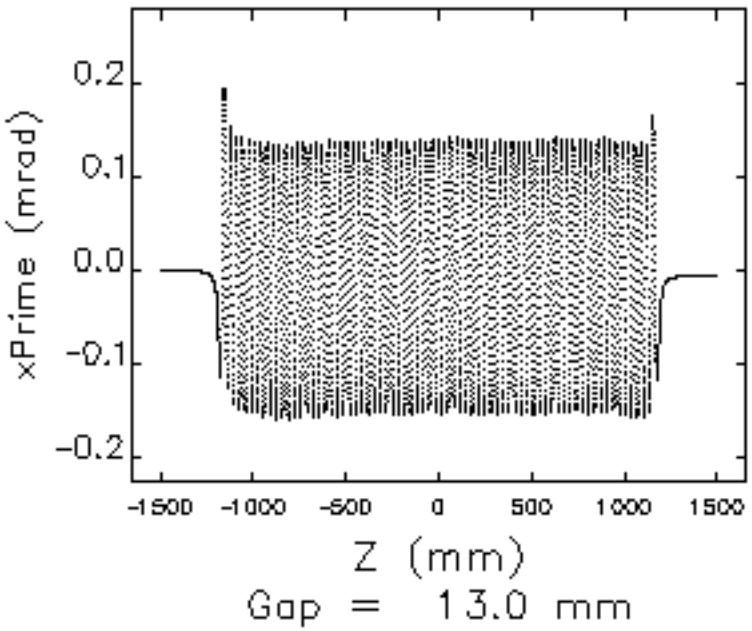

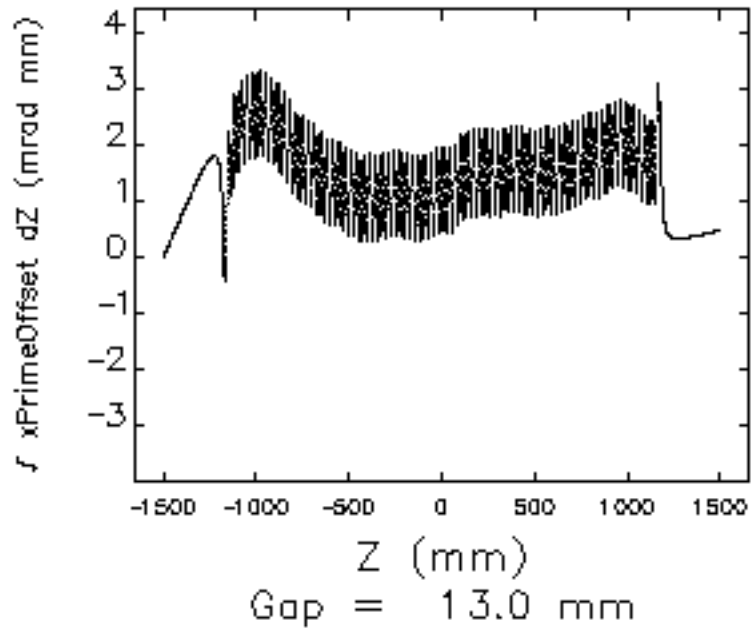

Insertion Device Magnetic Measurement Data and Field Integrals

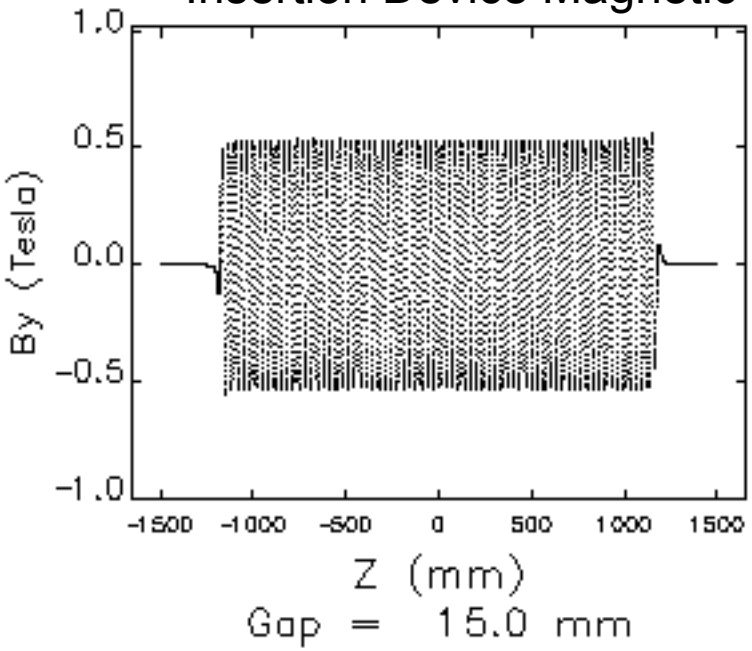

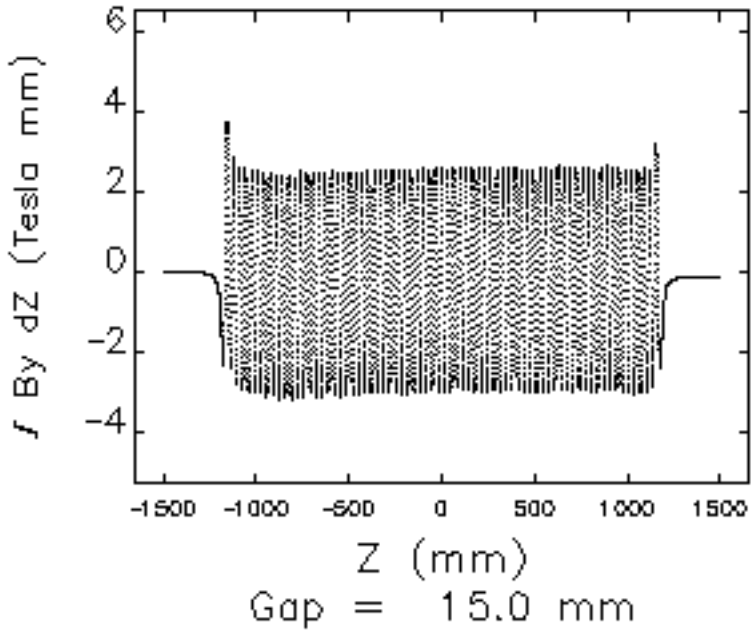

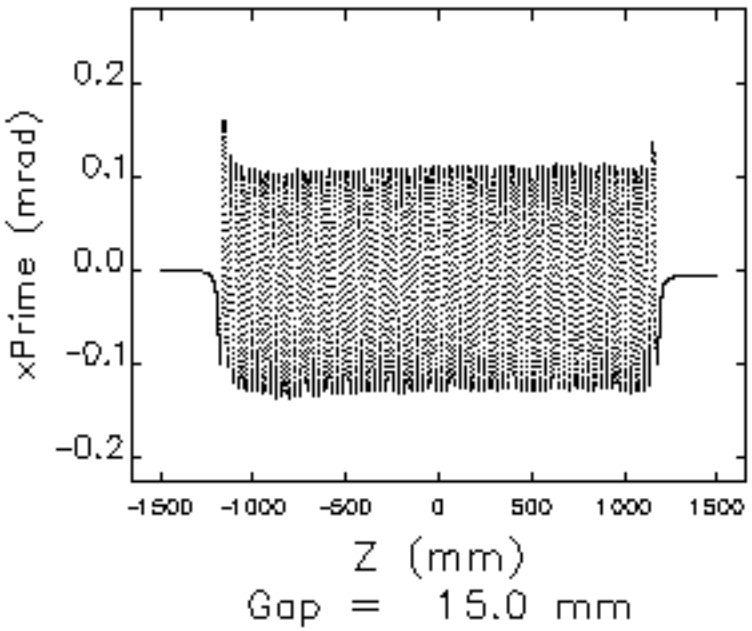

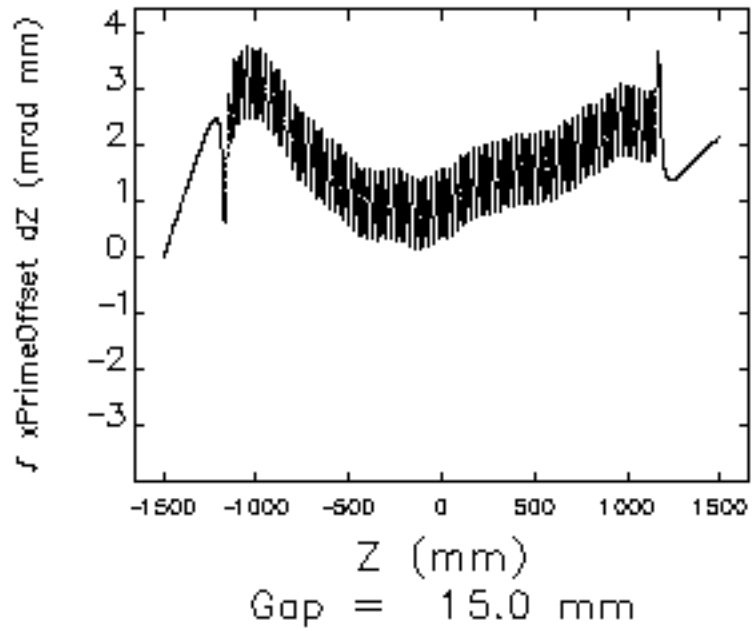

Insertion Device Magnetic Measurement Data and Field Integrals

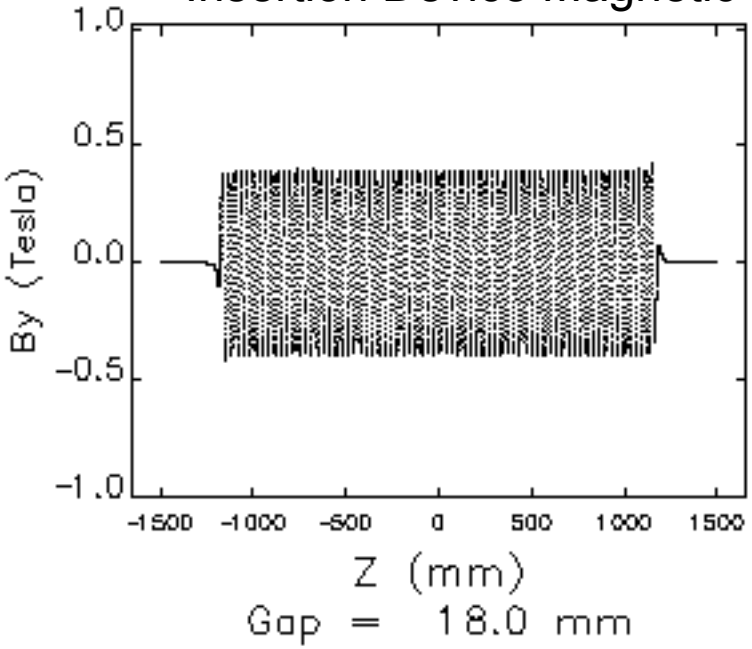

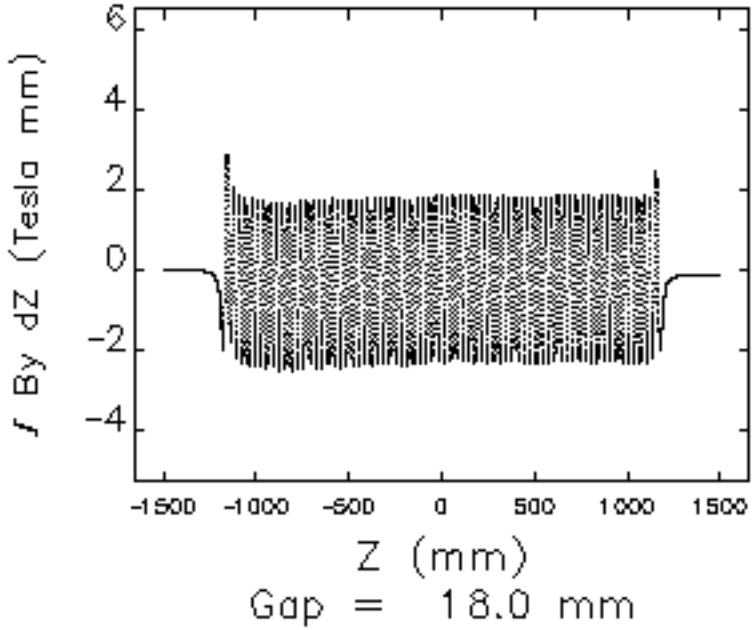

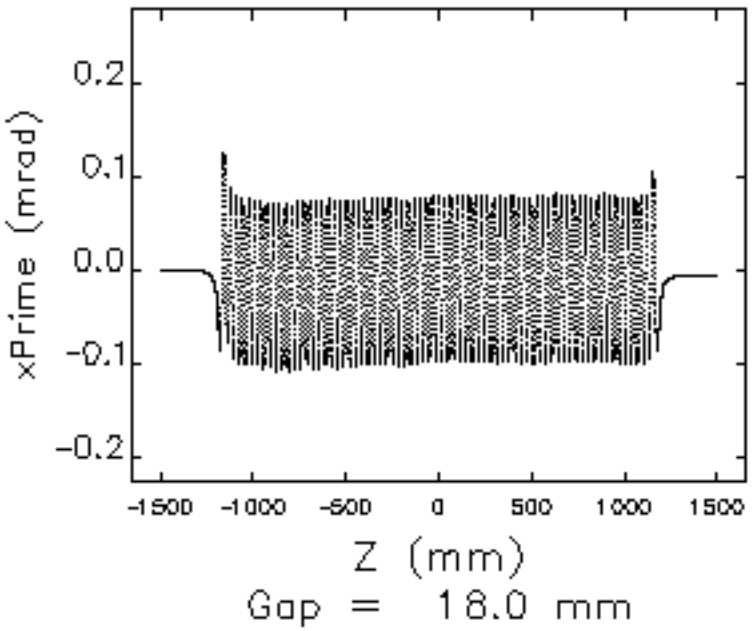

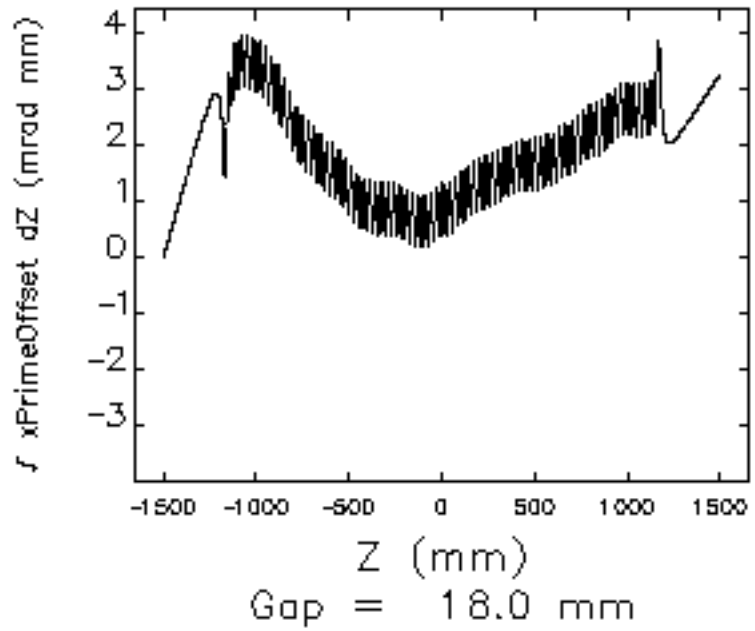

Insertion Device Magnetic Measurement Data and Field Integrals

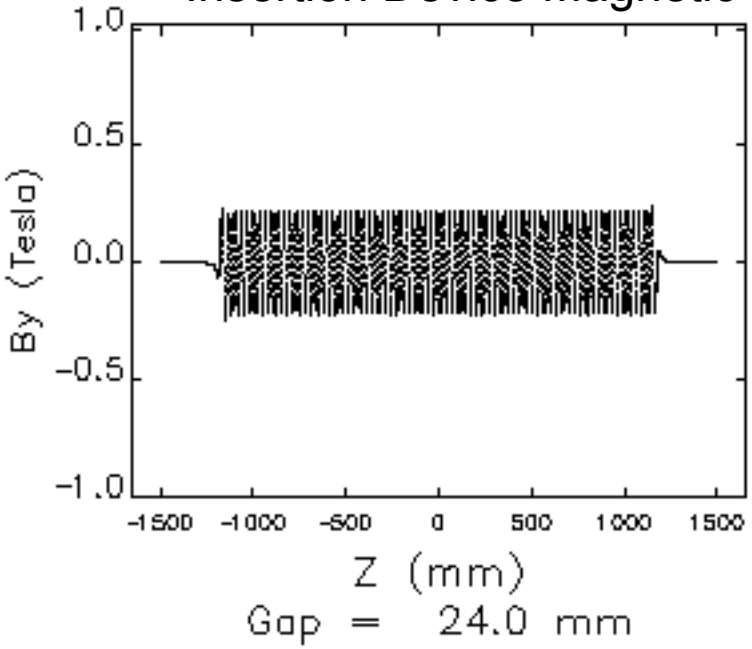

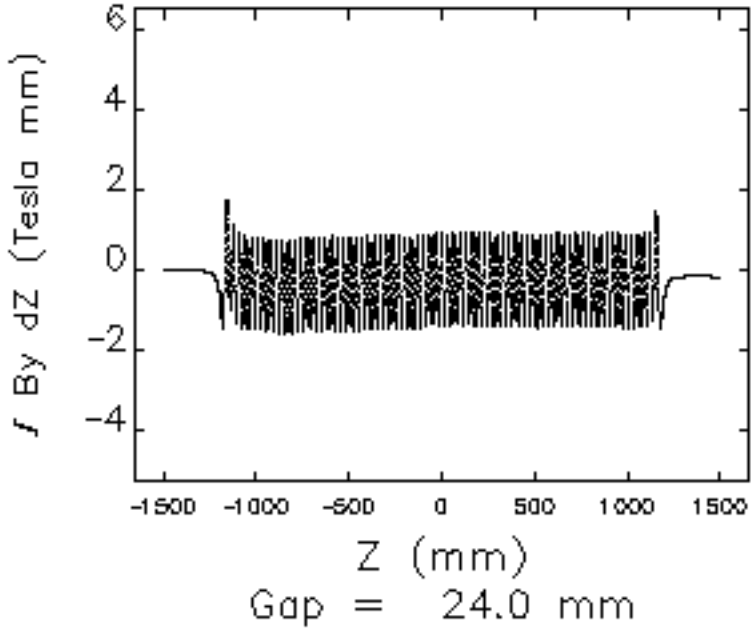

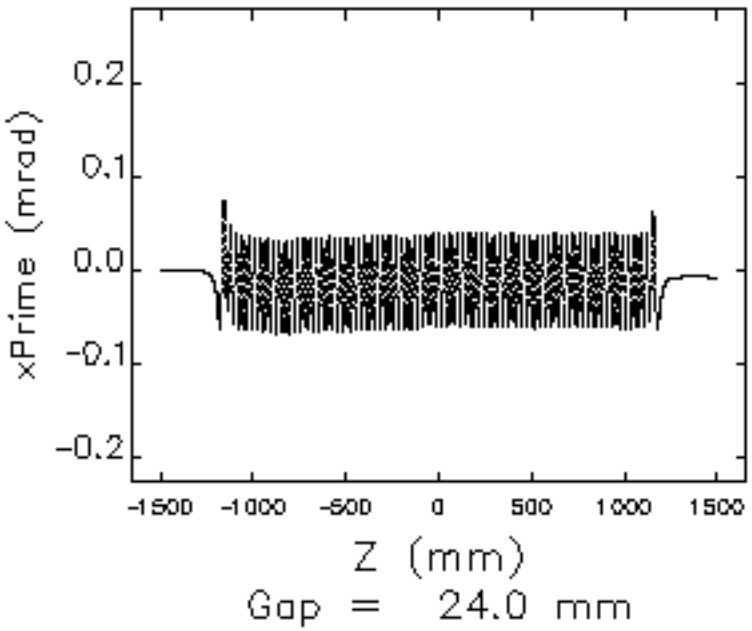

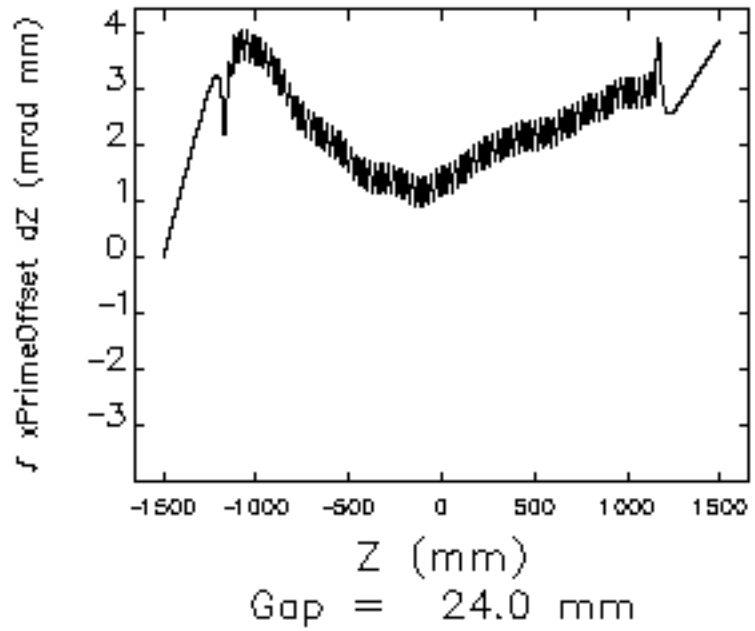

Insertion Device Magnetic Measurement Data and Field Integrals

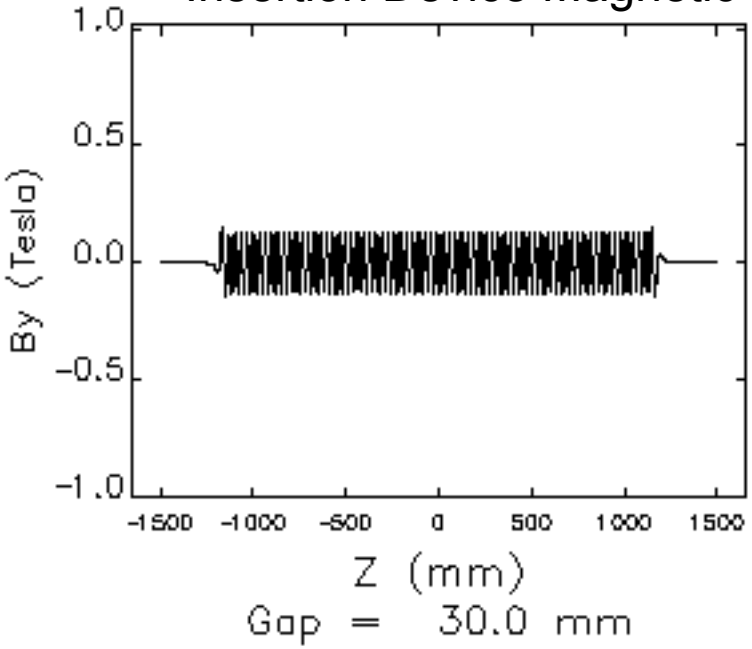

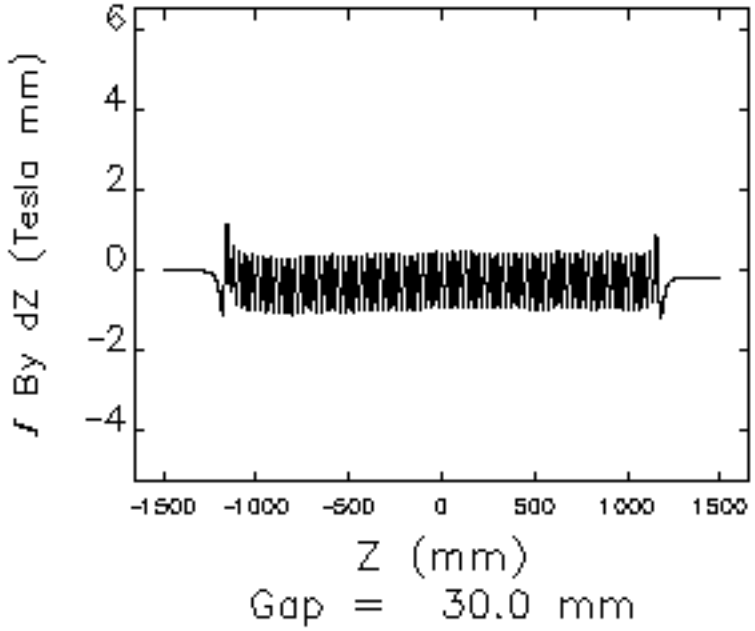

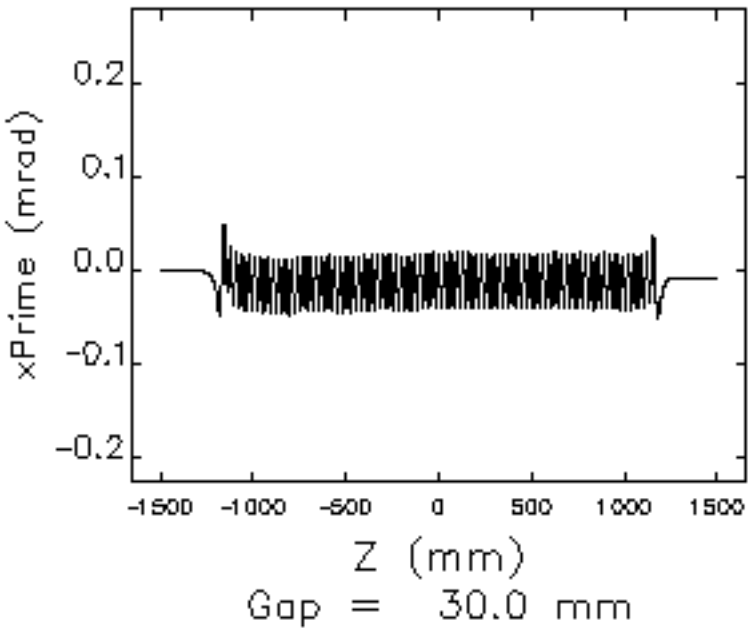

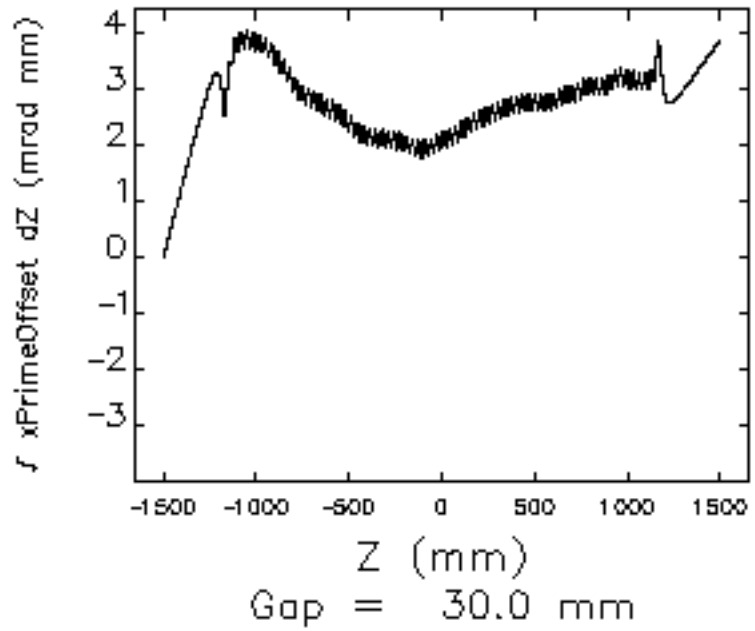

Reduction of ID gap change transient from reduction of orbit correction update rate

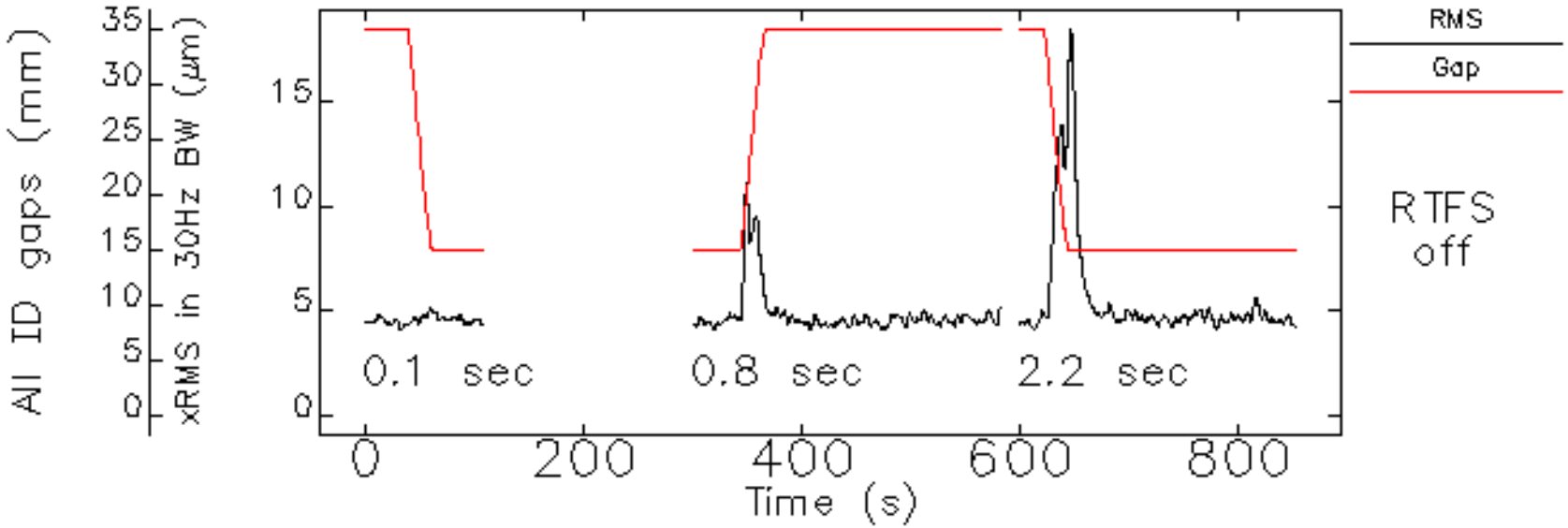

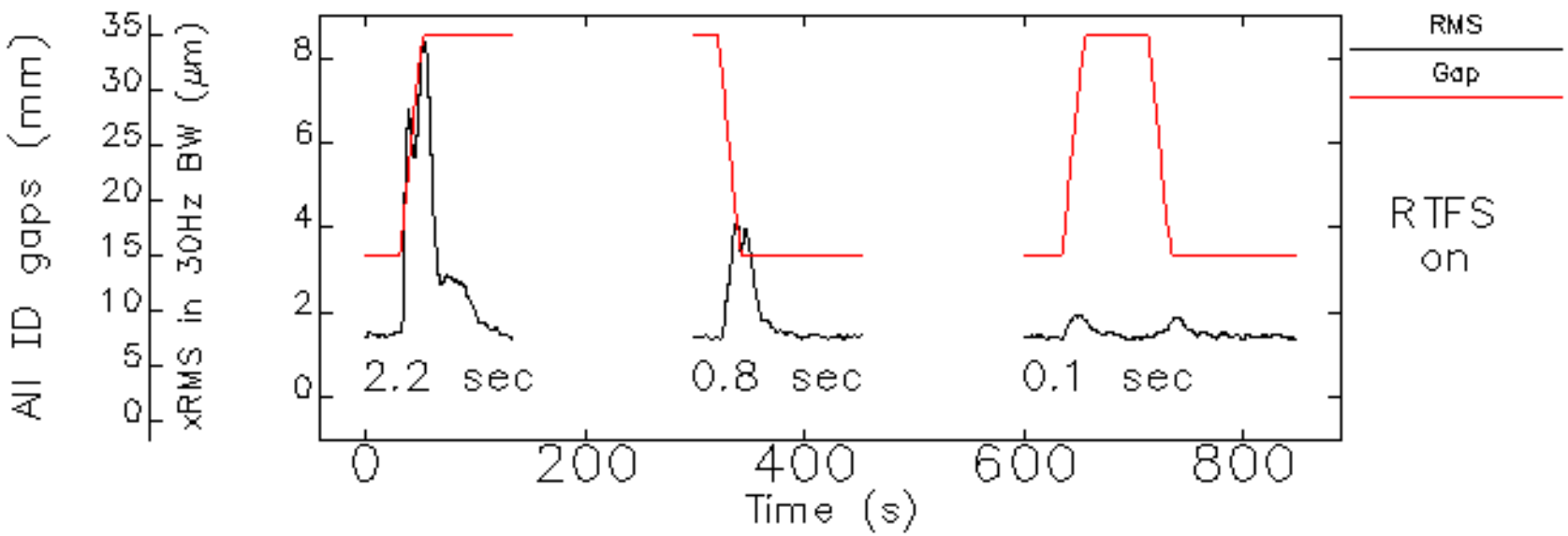

RF System

Thick metal vacuum chambers are an effective shield against most high frequency sources of stray magnetic fields. At the aps, the vacuum chamber is 0.5” thick, forming a very effective low pass filter with 3-dB point near a few Hz.

Exceptions are thin walled spool pieces associated with “fast” correctors (allows magnetic fields with frequencies up to a few hundred Hz to penetrate), and the injection pulsed magnets, either in-vacuum or with ceramic vacuum chamber.

The RF system introduces very large, very high frequency (100’s of MHz) electric fields into the environment of the charged particle beam.

Changes in rf frequency / phase are immediately seen as horizontal beam motion at locations in the ring where the dispersion function $\eta(s)$ is non-zero.

An Unhappy Master Oscillator

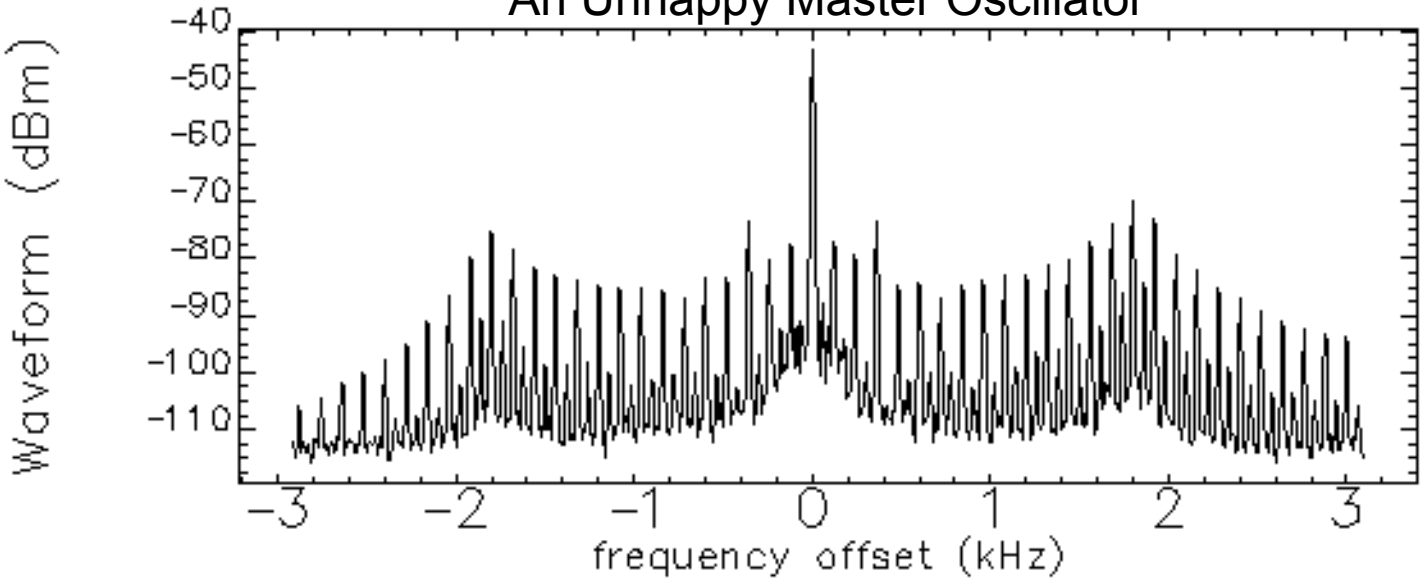
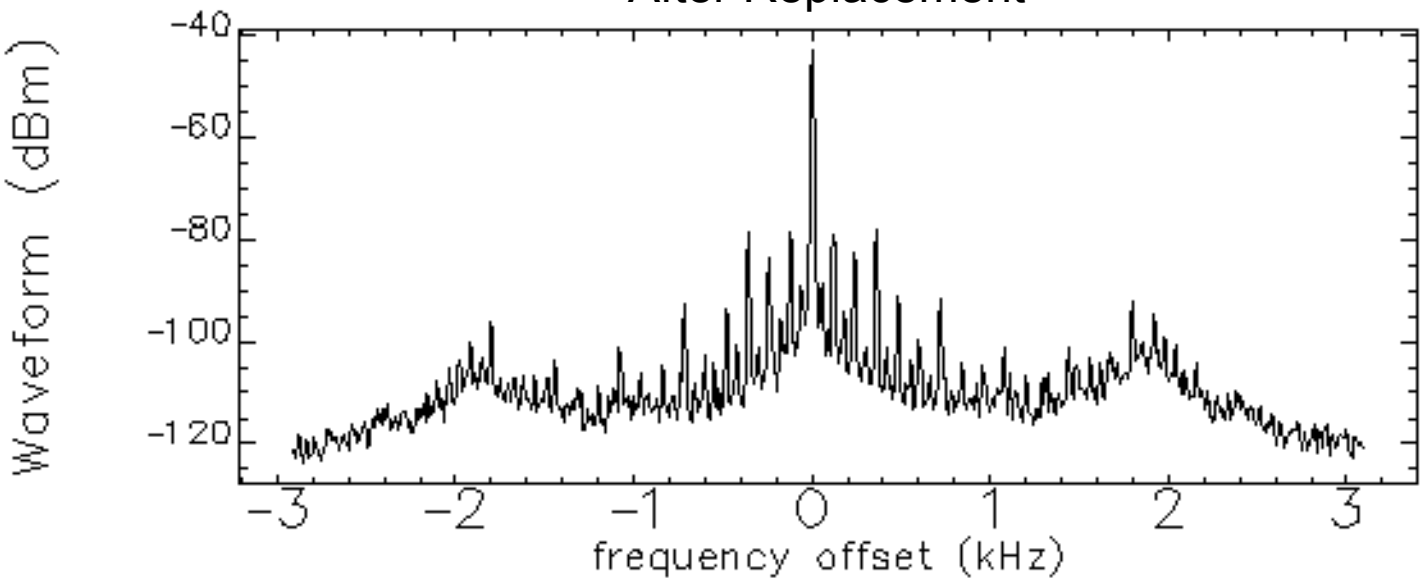
After Replacement